CODEN:LUTEDX/(TEIE-5352)/1-71(2015)

Industrial Electrical Engineering and Automation

Torque Sensor for Automotive Applications

An investigation of torque sensing techniques for drivetrain integration

Oskar Persson

Gustav Persson

Division of Industrial Electrical Engineering and Automation
Faculty of Engineering, Lund University

LUND
UNIVERSITY

Torque Sensor for Automotive Applications

An investigation of torque sensing techniques for drivetrain integration

Master Thesis by:

OSKAR PERSSON
GUSTAV PERSSON

oskar.nh.persson@gmail.com
gustav.persson90@gmail.com

Division of Industrial Electrical engineering and Automation (IEA)
at the Faculty of engineering at Lund University.

Supervisor: BENGT SIMONSSON
Examiner: GUNNAR LINDSTEDT

May 2015

Abstract

The use of sensors in the automotive industry is increasing, improving performance and safety of the vehicles. The ambition at BorgWarner TorqTransfer Systems AB is to increase torque accuracy to optimize their powertrain solutions. Different methods to measure torque on a rotating shaft is presented and evaluated.

The method that was selected was the magnetoelastic method. This method utilizes the effect where the magnetic properties changes in a material in response to mechanical stresses. A circularly magnetized ring divided into two oppositely polarized bands was press-fitted onto the main shaft of the coupling together with an isolation ring. When the ring is subjected to torque it generates a magnetic field that is dependent on the torque which is then measured using a magnetometer.

Two shafts were fitted with the sensor concept for testing, of which one shaft was weakened to get higher stresses in the sensing element. A series of test were conducted to measure the sensors response and sensitivity. The magnetoelastic material was tested before assembling the sensor, it showed a relatively linear dependency between stresses and magnetic field, within the tested range. The test result from the weakened shaft clearly shows the torque induced variations of the magnetic field. The proposed solution demonstrates the potential of making a compact sensor with few components with possibilities to be integrated in BorgWarner products.

Preface

This master thesis was done at BorgWarner TorqTransfer Systems AB in Landskrona Sweden with supervision from the Division of Industrial Electrical engineering and Automation (IEA) at the Faculty of engineering at Lund University. The authors have been working together with all the parts and contributed equally with the completion of the thesis. A special thanks to the following people for their support and advice:

CHRISTER EBBESSON	*As our mentor at BorgWarner he supported us during our time at the company.*
BENGT SIMONSSON	*Supervisor at IEA that provided us with input during the project.*
GUNNAR LINDSTEDT	*Examiner at IEA.*

Contents

Nomenclature

Abbreviations

RF-link ..... Radio Frequency link

AMR ..... Anisotropic Magnetoresistance

IDT ..... Interdigitated Transducer

Gen V ..... Generation V, Borgwarner's latest all-wheel drive coupling

AWD ..... All-Wheel Drive

ECU ..... Electrical Control Unit

Variables

K_u ..... Magnetic uniaxial anisotropy, the directional dependence of a material's magnetic properties

M_r ..... Remanent magnetization

H_c ..... Coercive force

μ_r ..... Relative permeability

M_s ..... Saturation magnetization

λ_s ..... Saturation magnetostricion

H_{easy} ..... Magnetic field along the easy axis

σ ..... Mechanical stress

1

Introduction

1.1 Background

As cars are getting more computer controlled, different sensors have an important role of providing the computers with information of the current state of the vehicle. Sensors monitors engine performance, the speed of the wheels are measured for the ABS and ESP system, they provide comfort and safety for the passengers etc. Today each vehicle has an average of 70-100 sensors on board and it is expected to increase to nearly 200 sensors per vehicle to 2018 [31].

The number and performance of the automotive sensors continues to grow, however the use of torque sensors are still limited. Commonly, the control scheme relies on models of the engine and transmission together with measurements of indirect parameters. Applications where torque sensors are of interest for the automotive industries includes measuring driveshaft torque, steering-wheel torque for electric power steering and engine output torque.

As the drive systems are getting more advanced and intelligent with functions such as torque vectoring, the ability to measure torque provided to each wheel are becoming increasingly important. With an accurate measurement of the torque applied to the wheels it would be possible to better control the power distributions between the wheels and limit the highest allowed torque. Knowing the maximum torque also makes it possible to further optimize components with regards to their strength and weight.

1.2 Objective

Torque and force sensors available today are most suited for measurements in industry and in testing applications and are not suited for the requirements of the automotive industry. The task is to identify methods to measure torque in the all-wheel drive couplings from BorgWarner. The report should provide suggestions for solutions that are tailored for high volume production and integration in the coupling. The sensor solution should be analysed in a test rig to validate its performance.

The goal is to improve the accuracy and reliability compared to the current method for torque measurement.

1.3 Scope

Torque can be measured either by doing measurement on the shaft subjected to torque, or a force that arises between other parts in the construction when a torque is applied. These forces can e.g. be reaction forces acting where the coupling is mounted to the car or forces between gears. A direct measurement will have the benefit of being less sensitive to disturbances compared to if it is a chain of forces of actions and reactions before the measurement takes place. Since reaction forces will be exerted on stationary parts, measuring them can be less complex compared to do the measurements on a rotating shaft.

Torque can be measured on other places in the drivetrain outside the coupling. However, since the goal of this project was to integrate in the coupling these alternatives were not further investigated. About 30 mm of the shaft inside the coupling is unobstructed from other components with some free space around it which gives the possibility to integrate a sensor around the shaft. In chapter 3.2 it will be shown in more detail.

It was decided the focus should be on developing a sensor concept for direct torque measurement placed in the free space around the rotating shaft.

1.4 Outline of the thesis

This thesis will describe the step by step development process of a torque sensor for BorgWarner Generation V coupling.

An investigation of different techniques and their variants of measuring torque are done in chapter 2, "Theoretical Background", where their functional principles and which physical properties they rely on are described.

In chapter 3, "Concept Development", the process of deciding which technique to be used is presented. The possibility of using sensors available on the market are investigated. This chapter will also cover the making of the prototype and which choices that were made when selecting parts and materials.

All the tests of the prototype and the test results will be presented in chapter 4 “Testing”. A test plan is given in which it is defined what kind of tests were made, how they were conducted and what information they were going to provide.

Results from the tests will be analysed in chapter 5, “Analysing results”. The performance of the prototype will be presented and determined if it reaches the specifications defined in chapter 3.

Further development of the sensor and changes that can be made to improve the performance is discussed in chapter 6, “Discussion”.

2

Theoretical Background

A series of sensor techniques used today for measuring torque on shafts are briefly explained. The working principles of the techniques and their properties were researched. These techniques will later be evaluated in chapter 3.3 to find the technique most suitable for the application.

2.1 Strain gauge

Strain gauge is a device that is measuring the strain in an object. It relies on the principle of a conductor changing its electrical resistance with strain. It usually consist of a flexible material on which a pattern of conductive foil is attached. This is then attached to the object of interest with some kind of adhesive. This makes the strain gauge deform with the object and thus strain occurs which causes the electrical resistance to change which then can be measured. The change in resistance in relation to strain is called gauge factor, this is typically around two [26]. The strain is usually not larger than a couple of millistrain and thus the changes in electrical resistance will be in the range of tenths of one percent. To be able to measure this small difference the strain gauge is often used in a bridge configuration, Figure 2.1.

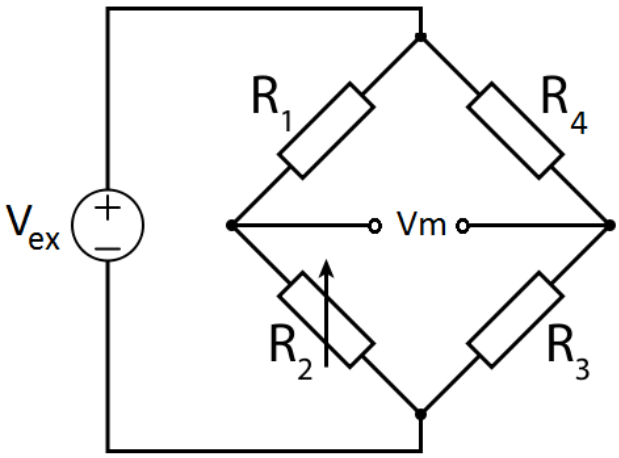

Figure 2.1: Strain gauge in a bridge configuration

The bridge is excited with a voltage V_{ex}, and the voltage is measured over V_m. If R2 is the strain gauge with the same unloaded resistance as the R_1, R_3 and R_4 the voltage over V_m is zero when there is no strain. In the loaded condition the resistance of R2 will differ from the other resistors, and a voltage can be measured over V_m. Thermal expansion of the specimen will cause the gauge

to produce an output signal as if there were tension in the specimen. To compensate for this the fixed resistor R3 can be replaced with a secondary strain gauge but placed 90° to the first strain gauge. A thermal expansion will affect both sensors equally and thus the resistance ratio between them will stay constant and the output signal will be less affected.

For torque measurement it is desirable to have the sensors mounted 90° relative to each other since the principal strains, compression and tension, will be perpendicular to each other. Compression will cause the resistance to decrease and tension will cause it to increase. Thus the strain induced resistance ratio, between the sensors, will change more compared to bending or pulling, resulting in a stronger signal.

Mounting of the sensor is critical to get a proper function. The surface needs to be free from any contaminations and accurately placed. Since the stresses are not usually uniform in all directions a misaligned sensor will cause error in the indicated stress[36]. When using strain gauges on a rotating shaft, the power supply to the sensor needs to be provided by slip rings or induction. The signal could also be transferred via slip rings but that is susceptible to wear. More commonly today is to transfer the signal wireless via an RF-link. This means more equipment has to be mounted on the shaft.

2.2 Magnetoelastic

The magnetoelastic effect or Villari effect is the change of the magnetic properties of a magnetic material subjected to mechanical stress [3]. The induced stress causes the spontaneous magnetization present in ferromagnetic materials to rotate from their initial orientation. The magnetic properties changes in the direction of the applied stress e.g. a material with a positive magnetostrictive constant subjected to tension will increase its permeability in the direction of the tension.

The inverse effect is known as magnetostriction and was first discovered by James Joule 40 years before Villari in 1842 [3]. It is the effect whereby ferromagnetic materials can change their dimensions when subjected to an magnetic field. If a ferromagnetic rod is subjected to an external axial magnetic field, the rod will increase or decrease in length depending on the sign of the magnetostrictive constant of the material. The magnetic domains that are randomly oriented in an ferromagnetic material align themselves parallel to the applied magnetic field as seen in Figure 2.2.

A closely related effect is the Matteucci effect. When a ferromagnetic rod is subjected to torque it creates a helical anisotropy of the susceptibility. As seen in Figure 2.3, rod A has a circularly magnetized field M_{rA} that under torsion T will create an axial field component. M_{rA} rotates towards the principal line of stress $+\sigma$ and gives rise to the formation of magnetic poles at the end of the rod. Similarly the remanent axial magnetization M_{rB} in rod B will under torsion create a circular field component.

In sensor applications, the magnetoelastic effect can be used to convert mechanical energy to magnetic energy. The changes in the magnetic properties that occur in the material when stress is applied can be measured with a magnetic field sensor. It means that magnetoelastic torque sensors can measure e.g. the torque on a rotating shafts entirely contactless. The shaft that is subjected to measurement does not need any power supply or electronics attached to it, all the electronics

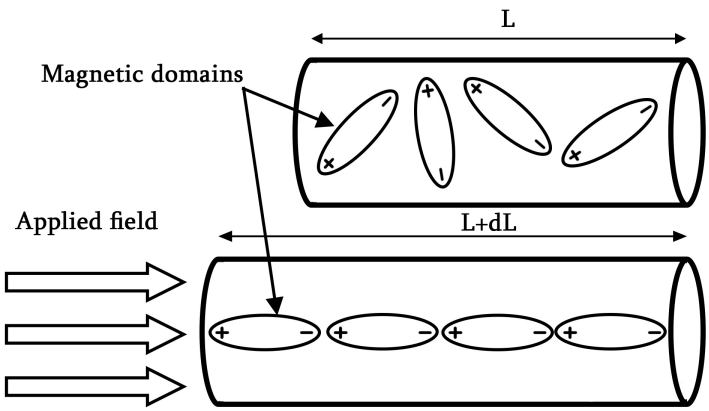

Figure 2.2: A ferromagnetic rod changes in length due to magnetostriction

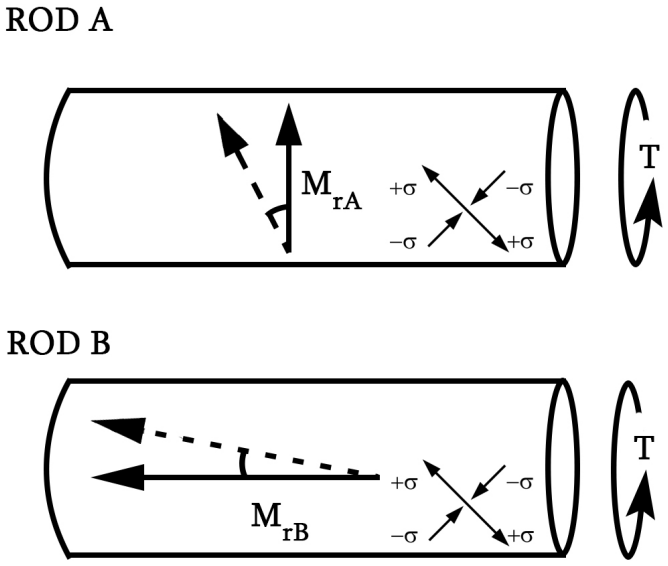

Figure 2.3: The Matteucci effect on a magnetized rod

can be placed stationary in the housing. There are two main types of sensors for measuring the torque due to changes caused by the magnetoelastic effect , the “Induction based” sensors and the “Polarized band” sensors.

2.2.1 Induction

In its basic form the induction based sensor is a U-shaped transformer core with one coil around each leg. The U-core transformer element is placed in proximity to the magnetostrictive sensing element that is subjected to stress with a typical air gap of 0.5-1.0 mm as in Figure 2.4. The primary coil V_1 induces a magnetic flux that is coupled with the sensing element and in the secondary coil V_2 a voltage is induced depending on the strength of the flux. In accordance with the magnetoelastic effect the permeability of the sensing element will increase or decrease depending on the strength and direction of the stress. This affect the amount of magnetic flux that passes through the element and the torque that is applied to the shaft can be measured in a non-contact manner.

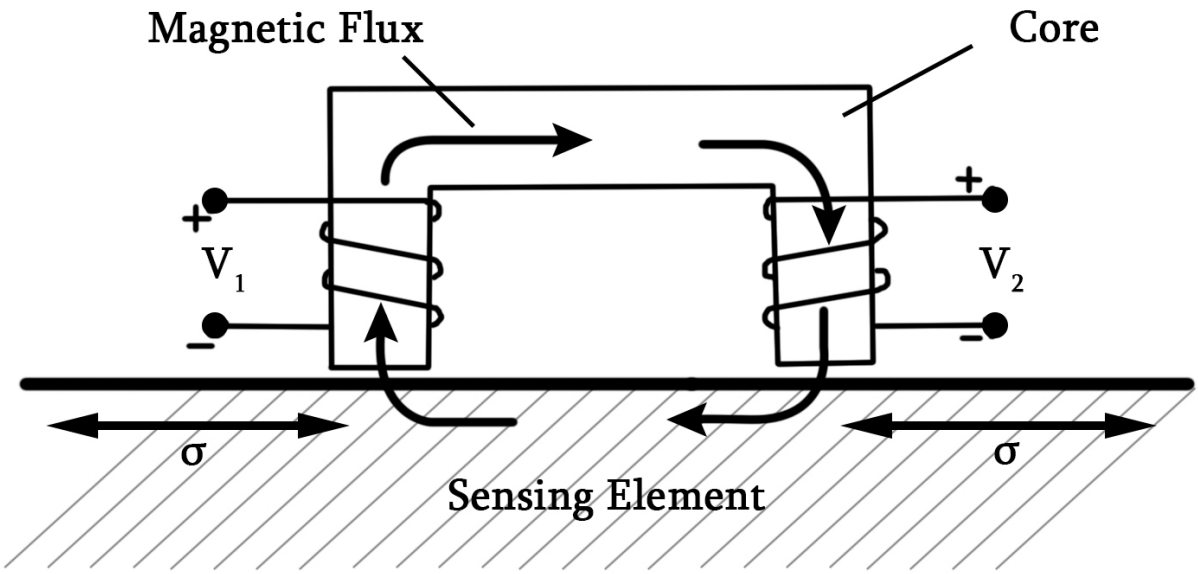

Figure 2.4: The basic principle of induction based magnetostrictive sensors

There are three major types of designs for the induction based sensors, Branch, Cross and Solenoid designs. The following sections will cover an overall description of the major designs. For a detailed comparison of the different designs and analyses of the equivalent magnetic circuits, thorough research has been done by William J. Flemming [11].

Branch Design

The branch design consist of one common primary coil and two or four secondary coils as can be seen in Figure 2.5. The legs of the sensor are placed in the shape of a V or an X and the excitation coil E_A is placed on the middle leg. The rest of the legs are for the secondary coils S_1-S_4 and they are oriented with a $\pm 45^\circ$ to the shaft which lines them up with the principle lines of stress due to applied torque.

The primary coil induces a magnetic flux in the sensing element that is picked up by the surrounding legs. When no load is applied to the shaft an equal amount of current will be induced

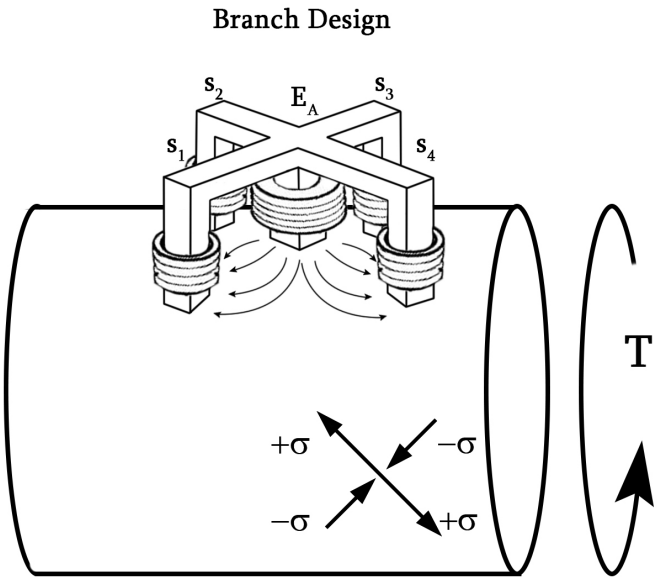

Figure 2.5: Principle sketch of the branch design

in the sensor legs. When the shaft is subjected to torque the permeability of the sensing element changes and the induced current increases in one of the principle lines of stress and decreases in the other. This voltage difference can be amplified and used as a measure of torque.

Cross Design

The cross design consists of two separate U-core transformer element with a coil on each one as in Figure 2.6. They are placed on the shaft perpendicular to each other with one of them parallel to the shaft. The primary coil E_B is supplied with an alternating current to generate a magnetic alternating field in the surface of the sensing element. The excitation pole directs flux across the air gap and into the sensing element where it spreads out and then converges to return via the opposite pole of the U-core.

The magnetic field lines in the sensing element can be seen in Figure 2.7 [7]. The points A and B mark the position of the poles of the secondary coil S_B and the points N and S mark the position of the poles of the primary coil E_B. In Figure 2.7, a) shows the field for an unloaded shaft where both the secondary poles lies on the equipotential line and hence no current will be induced in the secondary coil. In b) it shows how the magnetic field twists due to the magnetoelastic effect and the points A and B now have different magnetic potential. This will result in an induced current in the secondary coil which corresponds to applied torque.

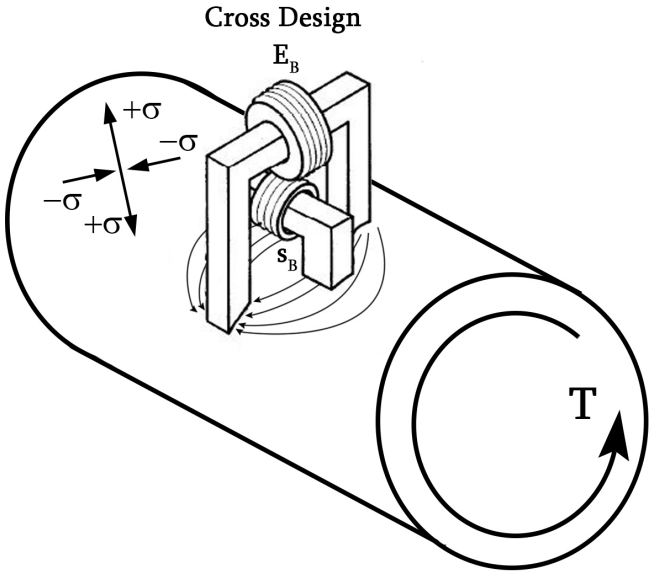

Figure 2.6: Principle sketch of the cross design

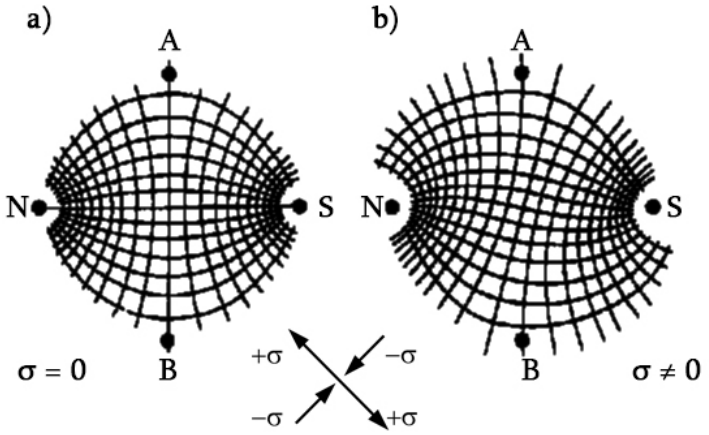

Figure 2.7: The cross design's magnetic field with and without applied torque

Solenoidal Design

The solenoidal design consist of a number of coils that encircles the shaft. The primary and secondary windings are located in the fixed sensing house with an thin air gap to the shaft. With this layout the height of the sensor house can be made smaller compared to the other sensors since it encircles the shaft. This means that in order to attach or remove the sensor, the shaft on which it measures torque needs to be disconnected. Applied on the surface of the shaft is a pattern with stripes directed at $\pm 45°$, which corresponds to the direction of the principle stresses. The pri-

mary coil is excited with an alternating current which induces a magnetic flux in the pattern of the shaft. The pattern concentrate the magnetic flux and reduces interference from inhomogeneities and residual stress in the surface material.

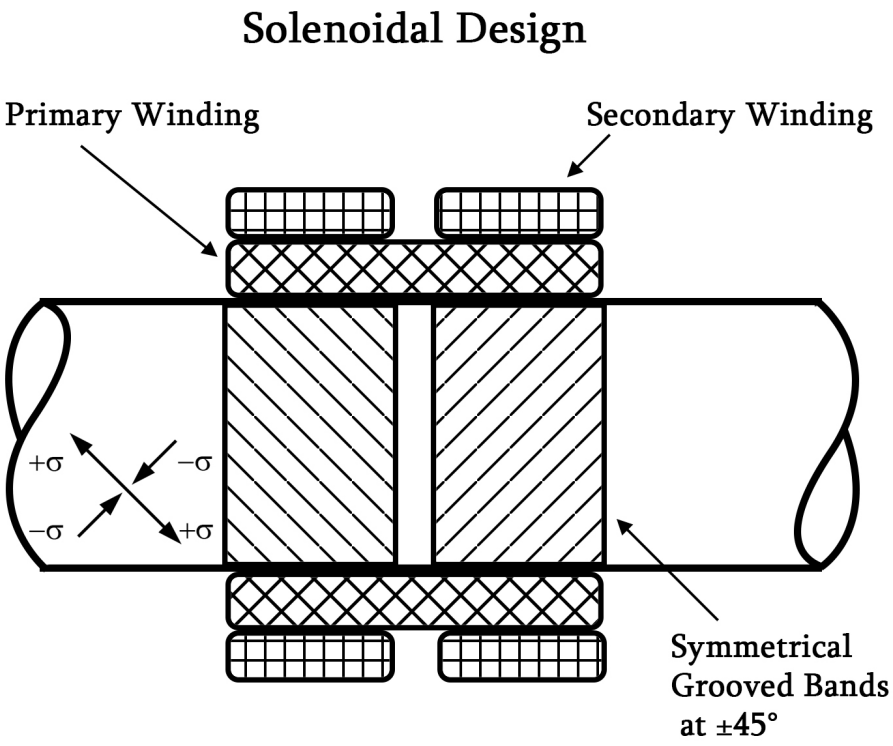

Figure 2.8: Principle sketch of the solenoidal design

2.2.2 Polarized band

This kind of transducer consist of a ferromagnetic sensing element with magnetostrictive properties together with a magnetic field sensor. The sensing element is circumferentially magnetized, creating a circular polarized band. This remanent circular magnetization M_r will ideally not generate any external field in the absence of torsional stress.

When torque is applied to the sensing element the magnetic anisotropy will shift to a helical orientation as shown in Figure 2.3. This tilting of M_r gives rise to an axial component of the magnetic field, resulting in an external field with magnetic poles at the axial edges of the element. One or more magnetic field sensors are then placed at close proximity to the poles as in Figure 2.9.

The core of the Polarized Band Sensor is the sensing element that is subjected to stress. The performance of the sensor depends largely on its properties. The shaft itself can be used as the sensing element, otherwise an external element can be attached to the shaft e.g. a ring that is pressed onto the shaft or a thin coating. The sensing element needs to be ferromagnetic with high

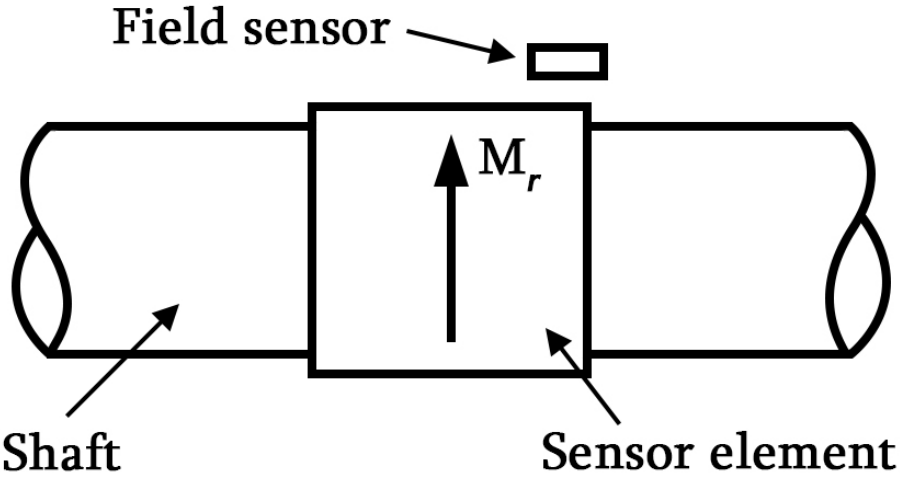

Figure 2.9: Elements of the polarized band design

remanence in order to contain the circumferentially magnetized field. Additionally the material needs a high magnetostrictive constant λ_s. The higher the constant, the greater the change of the magnetically properties under stress. Since the sensing element is passive and does not need any external excitation it can be power efficient. It can also be made small as both the sensing element and the field sensor requires little space.

2.2.3 Magnetic field transducer

Magnetic fields can be measured by variety of different sensing techniques. Different techniques are used depending on strength of the magnetic field and if they measure the vector or the scalar component[25]. Some techniques are more suited for laboratory use as they require cooling to cryogenic temperatures or the sample to be placed inside the magnetometer. Those type of sensors can be extremely sensitive and measure magnetic field down to fT (10^{-15}T). This sensitivity is 10^{11} times smaller compared to the earth's magnetic field. [34]. Sensors with a sensitivity adequate for measuring the change in magnetic field caused by the magnetoelastic material are commonly found in consumer electronics and are presented below.

Hall

A very common magnetic sensor is the hall effect sensor. It can be used as both an on/off switch or generate an output voltage proportional to the magnetic field. It works by the principle that a current will deflect from its straight path, due to the Lorenz force, when subjected to a magnetic field perpendicular to the current flow and the direction of the magnetic field. This will cause one side of the conductor to be more negatively charged and the other more positive and thus generate a voltage called hall voltage. This voltage is in the range of microvolt and needs additional electronics to be amplified to useful voltage levels. The sensitivity range of hall sensors are about 0.1

to 3000 mT. Hall sensors are commonly used in tachometers, ABS systems, proximity switching and so on. It is possible to sample a hall sensor at over 100 kHz [20].

Magneto Resistive

Magneto resistive sensors work on the principle that materials change its electrical resistance when subjected to an magnetic field. There are different versions of this sensing technique such as TMR (Tunnel magnetoresistnace), GMR (Giant magnetoresistance), AMR (Anisotropic magnetoresistance) CMR (Colossal Magneto Resistive) [27]. The different variations are used to measure different things such as magnetic field strength, direction and gradient. The change in resistivity varies greatly, from a couple of percent in AMR sensors to about 50 percent in CMR to 13 million percent in a semi-metal discovered as recent as 2014[2]. One of the common techniques are AMR sensors. They are commonly used for measuring earth's magnetic field in the compasses of smartphones. As its name suggest its sensitivity to magnetic field is not uniform and varies with the direction of the external field. This varying sensitivity makes it possible to arrange in a 3-dimensional way to get the vector component of the magnetic field. The sensitivity of AMR magnetometer are usually around one μT.

Fluxgate

The fluxgate consists of a core made of a material with high magnetic permeability with two coils wrapped around it, one sensing and one driving coil. The driving coils drives the core in and out of magnetic saturation. The core exists in different configurations but the most common ones are with a ring core or two parallel rods. When no external field is applied the two cores or the two halves of the ring will be driven into saturation at the same time but in opposite direction. The two fields cancel each other out and no current is induced in the sensing coil. When an external magnetic field is applied parallel to the magnetic field in the core it will aid it in one direction and oppose it in the other. This will cause one of the core halves to saturate faster than the other and they no longer cancel each other. This flux imbalance cause a current pulse to flow in the sensing coil which depends on both the polarity and magnitude of the field [21].

2.3 Surface Aucoustic Wave

Surface acoustic wave sensors or SAW for short is a micro mechanical device that takes an electrical input signal, converts it into a mechanical wave and then back to electrical again. The conversion is done by the piezoelectric effect which is a property of some crystalline materials where electrical charge accumulating in the crystal in response to mechanical stress. This effect works in both directions i.e. an electrical impulse causes the crystal to change shape as well as the shape change will cause a voltage. The mechanical wave is propagating at the surface of the chip, hence the name "Surface acoustic wave".

By converting the electrical wave to a mechanical it can easily be affected by physical properties such as stress, temperature or chemical deposition on the sensor. This allows the technique

to be used in a wide variety of sensing applications. However the most common usage of SAW-chip is as band pass filter in telecommunication applications where frequencies under and over the mechanical resonance frequency is attenuated.

If the SAW-device is used to sense strain it needs to be attached to the component with some adhesive, much like a strain gauge, to follow the tension and compressions of the material. To get a readout of the stresses, an electrical signal with a certain frequency is sent into the SAW-chip. The signal enters the sensor in an interdigitated transducer, IDT, where it is converted to an acoustic wave with the same frequency as the electrical wave but much shorter wave length due to slower propagation speed compared to the electrical signal. The acoustic wave travels about 5 orders of magnitude slower than the electrical. This IDT typically consists of thin film metallic "fingers" placed on the surface of the piezoelectric material using a photolithographic method [37], Figure 2.10.

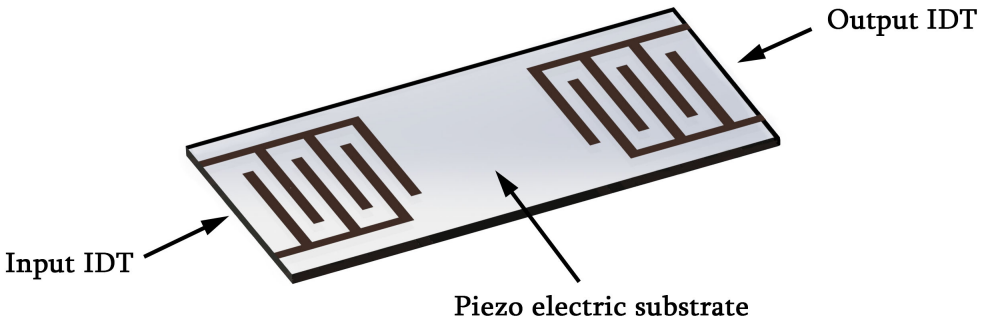

Figure 2.10: Two port SAW sensor

The frequency at which the SAW sensor operates is determined by this IDT pattern. The mechanical wave then travels through a zone which, because the slower propagation speed of the mechanical wave, is called delay line. It is in this zone where the wave is changed by the stress. The output signal can exit the sensor through the same IDT as it entered, called a one port sensor, or through another IDT, called a two port sensor. In a one port sensor the IDT is placed between two reflective gratings where a standing wave will form. This standing wave will resonate for a short time and generates an electrical wave as output. In a two port sensor, the wave propagates through the sensor to another IDT where it is converted back to an electrical wave. The output signal is compared to what was sent into the SAW device. Changes in amplitude, frequency or phase is used to determine the stress.

The electrical waves can be sent to the SAW device both wired and wireless. It does not need auxiliary power supply which makes it useful in wireless applications, only the energy in the signal is used. When used wireless, an antenna needs to be connected to the SAW-chip to pick up the signal and then transfer it back [23]. For a two port chip two antennas are needed. The ability to work wireless and without power supply makes it suitable for mounting on e.g. rotating shafts.

Torque sensors using this technique is not yet wide spread in consumer products. Mainly industrial and laboratory equipment where it sometimes is used as a replacement for strain gauges because of its possibility to operate without any electronics mounted to the shaft.

2.4 Displacement

Torque can be determined by measuring the difference in angle between two parts of the shaft caused by the twisting. This shift could also be converted to a linear movement and then measured by linear position sensors. Since the movements are often relatively small, mechanical amplifiers can be used to enlarge the deformations of the shaft.

2.4.1 Magnetic

In cars with electric power steering the torque needs to be known to apply the right amount of helping torque when steering. In hydraulic servo steering mechanisms it is done in a mechanical way with valves and torsion bars. In the electrical servo steering this is also done with a torsion bar, but instead of opening valves the rotational displacement of the torsion bar is measured and this becomes a measure of the torque applied by the driver. This displacement could be determined as in Moving magnets Technologies torque sensor [9] where a multi pole magnetic ring is attached to one end of the torsion bar and a sheet metal arrangement, with two parts magnetically isolated from each other, on the other end. These two metal parts conducts the magnetism from the magnetic ring to a hall sensor which is measuring the magnetic field. The intensity of this filed is changed when the magnets moves in relation to the metal arrangement and thus becoming a measure of the torque.

Bosch uses a similar technique [4] with a multipolar permanent magnet ring. Concentric to this ring is another ring with “windows” allowing the magnetic field to pass. Depending on how these two rings are rotated in relation to each other the magnetic field passing the “windows” will vary in intensity and is sensed by a hall sensor.

2.4.2 Optical

Light can be used in different ways to measure the torque applied to a shaft. On propeller shafts on ships, where large portions often is accessible, two rings can be attached to the shaft with a distance between them. The angular shift between these two rings can be measured optically where a light fixed to one ring shines on a sensor attached to the other, left shaft in Figure 2.11.

The circumferential shift of the light source compared to the sensor will give a measure of the torque. With a two dimensional sensor, shift in the axial direction can also be sensed which allows for measuring axial compression and tension as well, e.g thrust of a propeller [33].

Another way is to mount two rings on the shaft in which slots have been made, right shaft Figure 2.11. On each ring there is a device with a light emitter and a photo detector. When the shaft rotates the photo detector will give a varying signal depending on if the light is blocked or let through. When a torque is applied the rings will turn in relation to each other and the phase between the two signal will be shifted. This phase shift will be a measure of the torque.

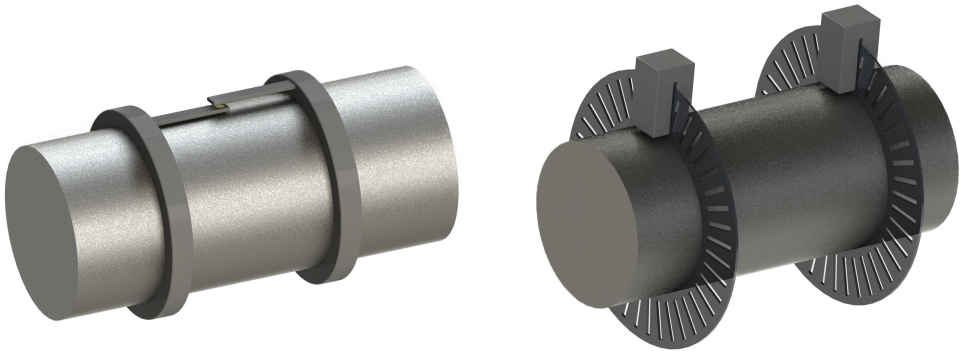

Figure 2.11: Optical displacement sensors

2.4.3 Capacitive

Capacitive sensors can be used as a non-contact distance sensor for conductive materials. By applying an electrical charge between two conductive plates the distance will be proportional to the capacitance. Capacitive distance sensor have the ability to measure distances down to nanometer level [5]. It is e.g. used in accelerometers where the position of micromechanical rods are measured to determine the acceleration [1].

2.4.4 Eddy current

Eddy currents are currents induced in conductive material when they are subjected to a varying magnetic field. The currents flows in circles perpendicular to the magnetic field. These eddy currents are then creating another magnetic field which is opposing the first field, thus there is an interaction between the conducting material and the source of the magnetic field [10].

The eddy current induced are dependent on the distance between the conductor and the source of the magnetic field sensors, this can be used to measure proximity or small distances like paint thickness or the radial movement of a vibrating shaft. These sensor have both an excitations coil which is creating the alternating magnetic field and a sensing coil which picks up the opposing magnetic field. The strength of this field is a measure of the distance between the probe and conducting material.

3

Concept Development

3.1 Existing torque sensors

The final torque sensor solution will be an integrated part of the coupling. A large portion of torque sensors on the market are usually aimed for industrial use and testing in laboratory environments. Finding a ready to use, commercially available sensor that fits the automotive industries specifications seems unlikely. In this section existing torque sensors for measuring torque on a rotating shaft is examined. The studied sensors will serve as an inspiration of working technical solutions in the development of this projects concept.

The commercially available sensors range from measuring just a few newton meters to several thousand newton meter. These sensors are usually expensive and not adapted for automotive specifications. The majority of them are strain gauge based sensors with wireless telemetry or slip rings encapsulated in a protective housing such as Transducer Techniques RST-series shown in Figure 3.1. SAW transducers are also found in sensors of the same type.

Figure 3.1: Transducer Techniques torque sensor

Simpler and a lot cheaper sensors have been developed for electric bikes. They are mounted in the pedal hub where they measure the torque applied on the pedals by the rider. This information is then used to determine how much assistance the electrical motor should give. The company Thun which is a manufacturer of bottom brackets for bikes produces a torque sensor, X-Cell RT Figure 3.2. It uses a shaft with magnetoelastic material and two fluxgate sensors to detect the changes in magnetic field.

Figure 3.2: Thun bottom bracket torque sensor

As mentioned in chapter 2.4.1, torque sensors are used for electrical power steering applications to determine how much the steering servo should assist the driver. Bosch's electrical power steering sensor, TSS (torque sensor steering) Figure 3.3 measures torque using angular displacement. It is measured by having permanent magnets on a torsion bar enclosed by a concentric ring with holes in it. These holes will let through more or less magnetic field depending on how it is twisted in relation to the permanent magnets. The magnitude of the field is sensed by hall sensors and they achieved a resolution of up to 0.002 [4] degrees.

Figure 3.3: Bosch electrical power steering torque sensor

As well as complete products, there are companies developing customized solutions according to customer specifications. Two such companies was contacted to investigate the possibilities of having a sensor custom made. However the estimated development cost was considered too high for this project and it was decided that the prototype should not be developed by another company.

3.2 Sensor specifications

The coupling that was provided for this project was BorgWarner's fifth generation all-wheel drive coupling called GenerationV Figure 3.4. GenV is BorgWarners's latest innovation in electrohydraulic clutch control and it automatically distributes power between the front and rear wheels.

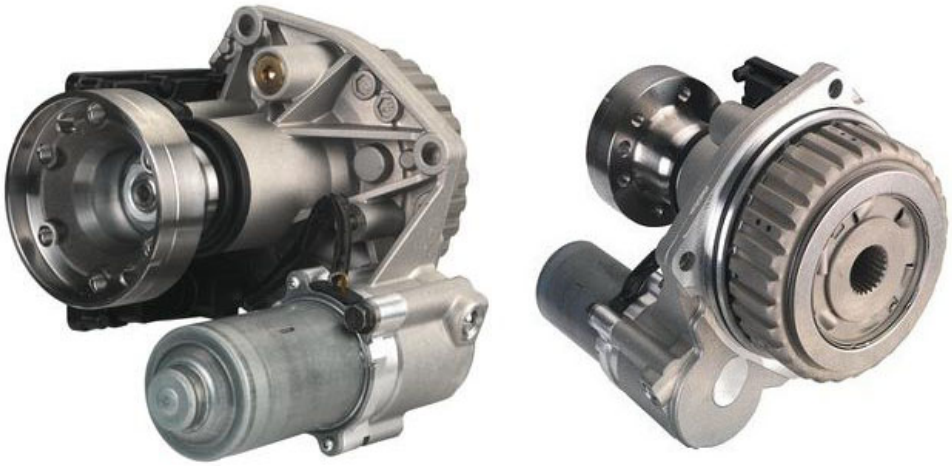

Figure 3.4: BorgWarner Gen V AWD coupling

As mentioned in chapter 1.3, the focus was on developing a sensor with direct torque measuring on the shaft. The model that was used for this research was a low torque GenV and an illustration of the available space is shown in Figure 3.5. Because the space can vary between different models the sensor should preferably be as small as possible to be able to fit other models as well. It is also easier to integrate the sensor when developing new couplings. The shaft is made of a medium carbon steel, the housing is made of aluminium and the space inside the coupling is partially filled with unpressurized hydraulic oil.

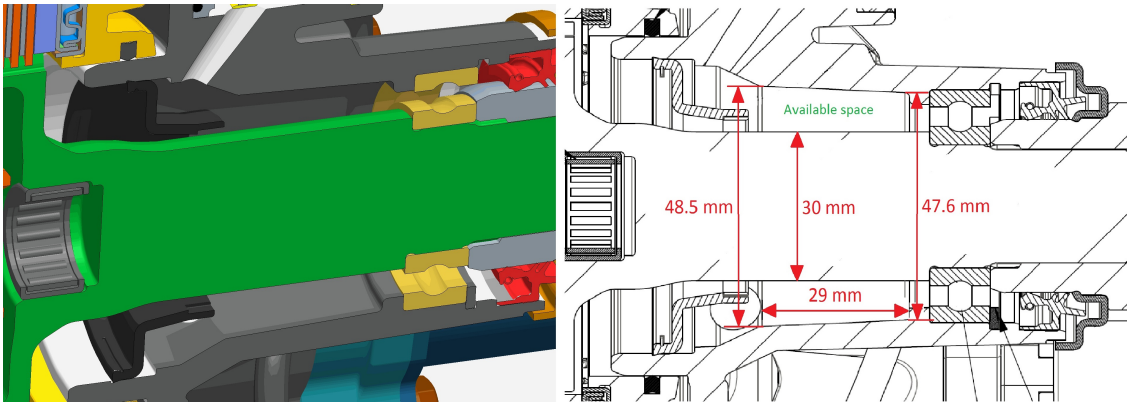

Figure 3.5: Space for sensor placement

The harsh environment inside the coupling and the tough demands of the automotive industries puts high requirements on the function and cost of the sensor. The sensor should be robust, to be able to operate in a wide temperature range and withstand vibrations. It should be reliable, provide accurate measurements and sense if the sensor fails. The main specifications of the sensor were identified and summarized in table 3.1.

Table 3.1: Sensor Specifications

Conditions	**Value**
Temperature	-40 - 125 $^{\circ}C$
Torque	2000 Nm
Accuracy	>95% (0-1000 Nm)
Measurement frequency	>1 kHz
Rotational speed	5000 RPM
Life span	Automotive standard
Operating environment	Unpresurized oil
Power consumption	<250 mW

In addition to the main specifications listed above a key factor is the cost. Since the goal is to integrate the sensor for high-volume production where every component is cost-optimized, the sensor needs to be cheap to produce. The resulting prototype of this research should aim to fulfill the main specifications. Lower performance is accepted since the prototype is subjected to further development and now it serves as a proof of concept.

3.3 Choice of sensing technique

When choosing the sensing technique for the drivetrain implementation, the previously discussed sensor principles were considered. Using a Strain gauge sensor on a rotating shaft that measures torque have two main disadvantages. First the sensor needs to be properly attached to the shaft with some kind of adhesive. Attaching the sensor is labour intensive and it is relying on adhesive bonding inside the harsh environment of the coupling. Secondly the sensor needs to be powered, either through slip rings or induction and the output signal needs to be transmitted via slip rings or an RF-link. Slip rings have the problem of wearing out and will not work in an environment with oil. Using a RF-link requires additional electronics on the rotating shaft which make attachment complicated.

The SAW sensor, which measures the resonant frequency change in the sensing medium needs to be attached to the shaft much like the Strain gauge. The process of attaching the sensor with adhesive onto the shaft was deemed inappropriate for high-volume production and of the four initial main principles the Strain gauge and SAW sensors was not considered to fit the application.

The principles that was chosen for further evaluation was the magnetoelastic and displacement principle. The magnetoelastic principle uses the effect were stress alters the orientation of the magnetic domains that are present in ferromagnetic materials. With this principle, the torque

can be measured by non-contact means on any shaft. If the shaft has inadequate magnetoelastic properties it can be fitted with a sensing element with the right characteristics.

The displacement principle measures the shift in position and when the shaft is subjected to torque it will twist with a small angle. The previously discussed displacement methods were compared to find the method that were the best fit for the sensor specifications. One of the specifications were that the sensor should be able to operate in the presence of hydraulic oil. Since the optical method requires unobstructed view between the emitter and the detector, the oil would interfere with the light and the method was discarded. One of the challenges with the displacement methods are how you transfer the angular shift of the shaft to the sensor in a non-contact way since having electronics on the shaft is undesirable. For the magnetic method this can be achieved by redirecting the changing magnetic flux with external flux collector to a stationary sensor as is done in [9]. For both the eddy current and capacitive principle the solution can be more difficult. In order for the sensor to be stationary mounted in the housing the angular shift needs to be converted to a linear movement.

Because of the magnetic methods more accessible way of transferring the angular shift it was considered for further development. The two main methods of the magnetoelastic principle was compared and evaluated against the specifications. The most promising method seemed to be the one based on polarized bands since it consumes less power than the induction based method which did not meet the power consumption specifications. In William J. Flemming's research on the induction based magnetoelastic torque sensor [11] he compares the output signal strength compared to the excitation voltage and frequencies. He shows that the signal decreases with decreasing voltage and frequency and the required excitation voltage and current would exceed the specified power consumption limit.

The two methods that qualified and seemed to meet the specifications were the magnetoelastic polarized band method and the magnetic displacement method. The magnetic displacement method that is currently used in steering-wheel torque sensors provides a non-contacting way of measuring the torque by measuring the twisting angle of the shaft. Given the small angle shift of the shaft during load the angle measurement system needs to be fine-tuned to get adequate resolution. The polarized band sensor with its few components of a magnetic field sensor and polarized bands attached to the shaft makes the method less complex. The simplicity of the construction and the recent development and research of integrating the sensor for automatic transmission applications [18][30][22] makes this a suitable method. With all the features of the magnetoelastic method with polarized bands it was selected as the primary sensing technique for this application. The magnetic displacement method was kept as a secondary option but for the limited scope of this report it was decided to only develop one concept into a prototype.

3.4 Sensor development

3.4.1 Sensing element

A number of different sensing element designs were considered. The easiest solution would be to use the shaft itself as the sensing element as it has been done in earlier research [32]. This principle has shown good linearity and reproducibility for a variety of materials but it sets high requirements on the homogeneity of the material and geometry. The material of the shaft requires good magnetic and magnetoelastic properties and common high strength steel have low magnetoelasticity [19]. The materials for magnetoelastic sensors are often high alloy steels. The properties of the medium carbon steel used in the given coupling was deemed inadequate which was verified after contact with a manufacturer of magnetoelastic sensors. Making a custom made shaft with another material was not an option due to limited time and resources of the project. The work was focused on attaching a sensing element on the existing shaft.

When separating the shaft and the sensing element the choice of material for the sensing element can be done more freely. The material can be optimized to have as good magnetoelastic properties as possible while shaft material can be optimized for its mechanical properties. One common difficulty when attaching the sensor element is to get a firm binding between it and the shaft hence appropriate measures should be taken to avoid interfacial slip.

The sensor element chosen for our concept was a magnetoelastic ring rigidly attached to the shaft. This approach provided a straightforward means to rapidly construct and test the feasibility of our concept. A common method of attaching a ring onto a shaft is by press fit. Press fit is a simple fastening method since it does not requires any bigger modifications of the shaft and it has shown promising results in earlier research [18]. Press fitting also creates a desired circumferential tensile stress in the ring which improves the magnetic properties by introducing a uniaxial anisotropy K_u in the direction of the magnetic bands[14]. The improved characteristics of K_u contributes to greater remnant magnetization and better hysteresis behavior.

It was decided to press fit one ring onto the shaft and with regards to the possible difficulty with interfacial slip another ring would be press fitted and secured with welds on a secondary shaft. This was done to be able to neglect the effect of slip. In addition to the magnetoelastic ring an intermediate ring was designed as a magnetic insulator between the shaft and the magnetoelastic ring. If the magnetoelastic ring was directly mounted on the shaft, approximately 90% of the generated magnetic flux would take the path through the shaft and would not be available for sensing the torque[18].

Another type of sensing element attached on the shaft is done by using the thermal spray technique. A thin coating of magnetoelastic material is deposited on a small area around the shaft by spraying molten or semi-molten particles onto the surface where the particles bond with shaft material. A magnetoelastic torque sensor utilizing this technique has been tested by Siement VDO [22]. With their design they claim to address some of the uncertainties such as long term stability, inhomogeneity of magnetic properties and scaling to high volume production. The thermal spraying technique seems promising and it was considered for our prototype but it was considered too time consuming and costly for the scope of this project.

3.4.2 Choice of material

The core of the torque sensor is the sensing element and selecting the right material is of great importance. The sensing element requires an alloy which combines good magnetic properties with mechanical strength. The sought mechanical properties of the sensing element are similar to the properties the shaft. It should optimally have the same modulus of elasticity, same thermal expansion coefficient and same or higher yield strength. If the modulus of elasticity is higher than the shaft, a larger part of the stress would go through the ring. Having an equal thermal expansion coefficient ensures that no stress is induced in the ring and the frictional bond stays the same with changing temperatures. A similar or higher yield strength is optimal for the ring to stay in the area of linear elasticity.

Of the magnetic properties, most emphasis is placed on the magnetostrictive coefficient λ as it directly affect the sensitivity of the sensor which is later explained in Equation 3.14. In addition, the remanent magnetization M_r and the coercive force H_c of the material is considered. M_r should be high to create a strong circumferentially directed magnetic field in the ring. H_c should not be too high which would make the sensor element hard to magnetize for the magnetization method described in chapter 3.4.6.

For the isolating ring between the shaft and sensor element, the sought mechanical properties are also those similar to the shaft. But for the magnetic properties it is desired to have as low relative permeability μ_r as possible.

The magnetostrictive coefficient is a property of ferromagnetic materials where it changes its dimensions when subjected to an external magnetic field. This property also affects the inverse effect where the magnetic properties change when subjected to stress. The magnetostrictive coefficient can be both positive and negative which affect how the material react in the direction of the field, Figure 3.6 [3]. For a positive coefficient, the randomly oriented magnetic domains in the material align with the field leading to an extension with the field and for a negative coefficient, the material contracts in the direction of the field.

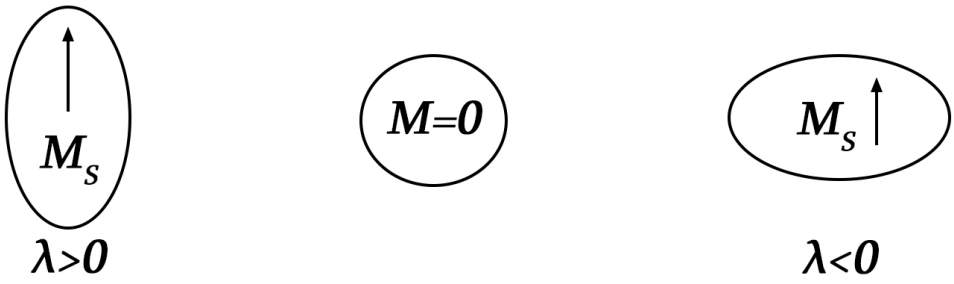

Figure 3.6: When subjected to a magnetic field the magnetostrictive coefficient determines the change in dimensions

The value of the magnetostrictive coefficient varies along the different crystallographic axis of the crystals in the material and is therefore anisotropic, Equation 3.1. For randomly oriented polycrystals the saturation magnetostriction coefficient λ_s can be written as [35]:

$$\lambda_s = \frac{2}{5}\lambda_{100} + \frac{3}{5}\lambda_{111} \tag{3.1}$$

Saturation magnetostriction is measured in microstrain (μS). Finding a defined λ_s for different ferromagnetic materials can be challenging since material data usually focus on the mechanical properties. After searching for a material that meet the above criteria and had a high λ_s the chosen material for the sensor element was EN 1.4021. EN 1.4021 is a martensitic stainless steel with high strength, good corrosion resistance and good magnetic properties. The mechanical data [6][24] and the magnetic properties [13][29] are presented in table 3.2.

The material chosen for the insulation ring was EN 1.4301. It is a common austenitic stainless steel with low permeability. This effectively reduce the magnetic flux from the sensor element from going through the shaft. Its properties [28] is also presented in table 3.2.

Table 3.2: Material parameters

Properties	**EN 1.4021**	**EN 1.4301**
Mechanical		
Modulus of elasicity E [GPa]	215	200
Yield strength $R_{p0.2}$ [MPa]	600	210
Tensile strength R_m [MPa]	800	520
Poisson's number ν	0.235	0.3
Thermal expansion coefficient α $[10^{-6} * K]$	11	15
Magnetic		
Saturation magnetostriction λ_s $[\mu S]$	20	-
Permeability μ_r	450	1.3
Coercive force H_c [A/m]	800	-
Remanent magnetization M_r [T]	0.82	-

3.4.3 Calculating ring parameters

The nominal dimensions of the rings Figure 3.7 are partly determined by the space available and partly by the function of the sensor. The length was set to 30 mm for both of the rings.

In order to allow twisting of the magnetoelastic ring the radial thickness of the isolating ring should be small, but with regards to prevent magnetic field from leaking into the shaft and not reach the sensor it should be large. The magnetometer will be about one millimetre away from the ring. To make the distance between the ring and magnetometer smaller than the distance between the shaft the ring, a thickness of 2 mm for the isolating and 1 mm for the magnetoelastic ring was chosen.

To prevent any slip between the rings and the shaft the attachment needs to be rigid to get the shaft and ring to behave as one part. To reduce the chances of slip occurring on the sides, reinforcing flanges are made to increase the contact pressure. With only friction transmitting torque

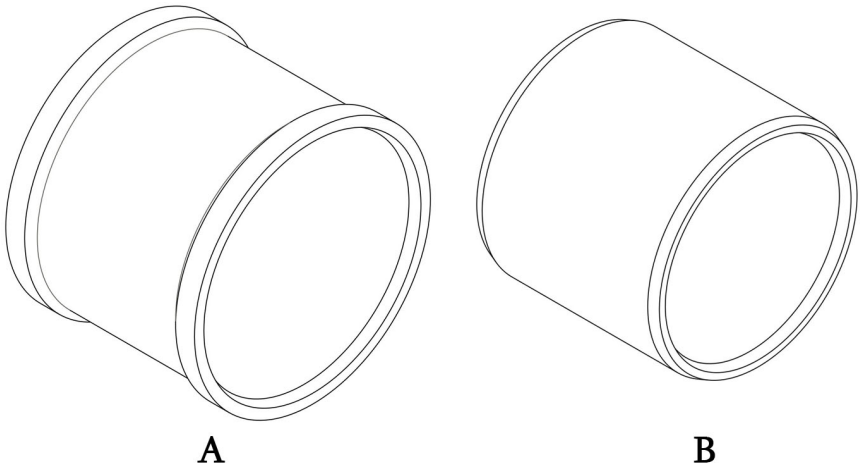

Figure 3.7: Magnetoelastic ring A and Isolating ring B

to the ring the contact pressure needs to be able to create frictional forces greater than the force needed to twist the rings the same amount as the shaft. If the fit is too tight undesirable yielding will occur during the pressing procedure. To know how much force is going to be transmitted through the frictional bond the ratio between the torque transmitted through the shaft and rings needs to be known. This is determined by the torsional stiffness and the shear modulus of the shaft and the rings, and is calculated in Equation 3.2 to 3.8. Material parameters are given listed in table 3.3.

Table 3.3: Material parameters

Part	**Modulus of elasticity E [GPa]**	**Poisson's number ν**	**Shear modulus G [GPa]**
Shaft	210	0.29	81
Isolating ring	200	0.3	77
Magnetic ring	215	0.235	87

$$\varphi = \frac{ML}{GK} \qquad K = \frac{\pi d^4}{32} \qquad G = \frac{E}{2(1+\nu)} \tag{3.2}$$

$$\varphi_{rings} = \frac{(M_{iso}+M_{mag})L}{G_{iso}K_{iso}+G_{mag}K_{mag}} \qquad \varphi_{shaft} = \frac{M_{shaft}L}{G_{shaft}K_{shaft}} \tag{3.3}$$

$$\varphi_{rings} = \varphi_{shaft}$$

$$\Rightarrow \frac{(M_{iso}+M_{mag})L}{G_{iso}K_{iso}+G_{mag}K_{mag}} = \frac{M_{shaft}L}{G_{shaft}K_{shaft}}$$

$$\Rightarrow \frac{M_{iso}+M_{mag}}{M_{shaft}} = \frac{G_{iso}K_{iso}+G_{mag}K_{mag}}{G_{shaft}K_{shaft}} \tag{3.4}$$

$$G_{mag}K_{mag} = 87*10^9\frac{\pi(0.0355^4-0.0335^4)}{32} = 2.81*10^3 \tag{3.5}$$

$$G_{iso}K_{iso} = 81*10^9\frac{\pi(0.0335^4-0.0295^4)}{32} = 3.8*10^3 \tag{3.6}$$

$$G_{shaft}K_{shaft} = 81*10^9\frac{\pi(0.0295^4)}{32} = 6.47*10^3 \tag{3.7}$$

$$\frac{M_{ring}}{M_{tot}} = \frac{G_{iso}K_{iso}+G_{mag}K_{mag}}{G_{shaft}K_{shaft}+G_{iso}K_{iso}+G_{mag}K_{mag}} \approx 0.51 \tag{3.8}$$

The two rings together will take 51% of the torque. Of the maximum allowed torque of 1350 Nm the coupling is rated for, 662 Nm will be going through the shaft and 688 Nm through the rings. The torque is assumed to be transferred through half of the surface area inside the ring since it also needs to be transferred back to the shaft. A diameter of 30 mm and total length of 27 mm, chamfers on the edges removes 3 mm from the originally 30 mm length, gives a total inner surface area of 2544 mm^2. The smallest surface pressure needed to transfer 688 Nm with half of this surface area, 1272 mm^2, is given by Equation 3.9. The frictional constant between steel and steel varies depending on different factors. For these calculations a static frictional constant of 0.6 [12] is going to be used.

$$\begin{aligned} T &= area*pressure*frictionalconstant(static)*radius \\ &\Rightarrow 688 = 0.00127*pressure*0.6*0.01475 \\ &\Rightarrow pressure = 61MPa \end{aligned} \tag{3.9}$$

With an inner pressure of 61 MPa the tensions in the wall will according to the Young-Laplace Equation 3.10 be 300 MPa where p is the inner surface pressure, r is the inner radius and t is the wall thickness.

$$\sigma_\varphi = \frac{pr}{t} \rightarrow \frac{61*0.01475}{0.003} = 300MPa \tag{3.10}$$

This is over the yield strength of about 210 MPa for the austenitic inner ring, but the yield strength of the outer ring is about 600 MPa and will likely prevent yielding. The effect of yielding in the outer magnetic ring is not known. Yielding of the isolating ring will most likely not have any effect on the magnetically insulating properties.

To calculate the tolerance zone that gives the surface pressure calculated before, as well as the pressing force required to press the rings on the shaft, formulas from the book "Kostruktionselement och maskinbyggnad" was used [8]. The two rings are approximated as one part with a 3 mm wall thickness during these calculations. They are going to be pressed together with one hundredth

of a millimetre interference fit to make them firmly attached but not enough to have a large effect on the inner diameter where the shaft is going to be pressed on. Since it is not totally clear if the frictional constant used is right, a tolerance zone that gives a minimum surface pressure of 76 MPa was chosen. This corresponds to +41/62 μm larger diameter of the shaft and -33/52 μm smaller hole diameter of the inner ring. The nominal value is 29.5 mm. This will require a maximal pressing force of about 6-10 kN. In Equation 3.11 the axial pressure on the ring is calculated to 90 MPa. This is well below the yield strength of the rings.

$$\frac{Force}{Area} = pressure \Rightarrow \frac{10 * 10^3}{3.06 * 10^{-4}} = 90MPa \tag{3.11}$$

3.4.4 Alternative ring attachments

There are multiple ways of attaching the ring to the shaft. The chosen method of pressing appears as the simplest way of doing it. However uncertainties of the friction and thus the ability to transfer force through this interface makes it hard to know if slip will occur. By physically locking it to the shaft ensures that any deformation in the shaft will be transferred to the ring and give rise to stresses.

Welding the sides of the ring to the shaft is one way of achieving a physical lock. The heat from the welding process might cause the temperature to rise to much which will change the metallurgical structure of the magnetic ring to a structure with worse magnetic properties. Cooling of the shaft might be required, or alternatively spot weld at some places around the circumference and thus not cause the temperature to rise over critical values.

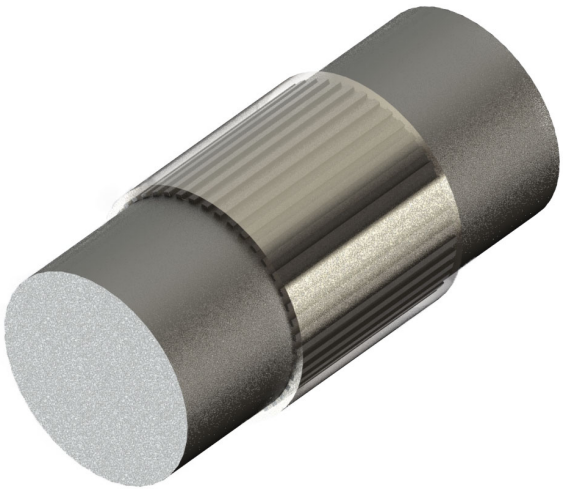

Figure 3.8: Spline ring attachment

Using splines on the shaft and the ring that is press fitted onto the shaft Figure 3.8. Splines could be made over the whole length of the ring or just along the edges. If splines are made just along the edges the ring could have a larger inner diameter in the middle to give a clearance

between the shaft and the ring to decrease the magnetic flux leaking into the shaft and thus not reaching the sensor.

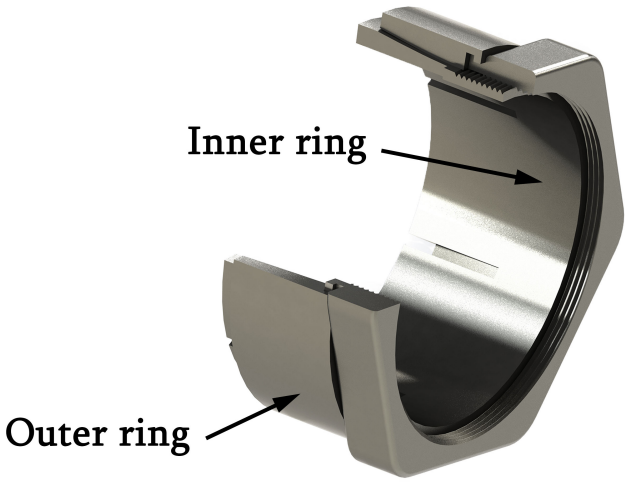

Figure 3.9: Trantorque

With a device like Trantorque Figure 3.9 where two oppositely conical rings with axial slots allowing for slight radial movement can be used to fasten a sleeve to a shaft. When the nuts are tightened the cones are pulled together and compresses around the shaft as well as expanding the sleeve and locks them together. One of these attached on each side of the ring would make the ring twist together with the shaft.

The press fit could be improved with regards to slip. The shaft can be cooled and the ring heated during the assembly process which would give a tighter fit. If the ring is heated, care must be taken not to heat it over the temperature where its magnetic properties changes. An alternative to heating and cooling is to use adhesive e.g. bearing mounting fluid to glue the two parts together.

3.4.5 Polarized band design

The parameters affecting the performance of the polarized ring sensor element are complex and depends on a variety of different factors like material, geometry and magnetizing method. Several researchers have studied the underlying principles of the magnetoelastic effect in order to get a better analytical model. It is shown in Figure 3.10 [17] that a ring with a remanent magnetic field M_r orthogonally to the axis will tilt with an angle θ_T when torque is applied to the shaft.

The principle shear stresses in a ring loaded only with torsion are oriented at a $\pm\pi/4$ helical angle around the shaft where $+\sigma$ is the tensile stress and $-\sigma$ is the compressive stress. For small angles of θ_T, M_r will tilt towards the $+\sigma$ helix and the angle can be expressed by Equation 3.12

$$\theta_T = \frac{3\lambda\sigma}{2K_u + N_d {M_r}^2} \tag{3.12}$$

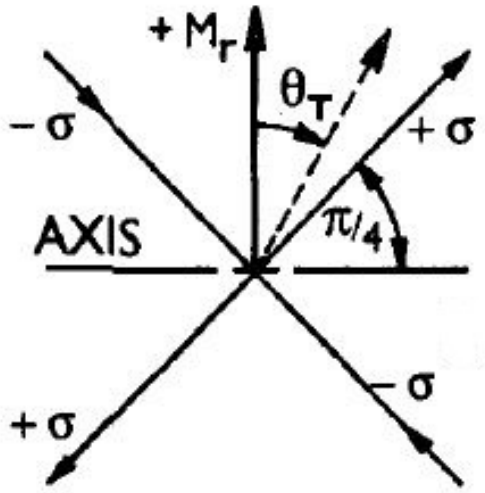

Figure 3.10: Tilting of the remanent magnetization M_r towards the tensile stress $+\sigma$

where N_d is the demagnetizing factor, an assumed constant factor based on the rings geometry and K_u which is the circumferentially directed uniaxial magnetic anisotropy. A magnetoelastic ring exhibits K_u in the circumferential direction which also is its easy axis H_{easy} based on the shape and typically the circumferential stress associated with press fit [16]. The axial component of M_r associated with this tilt is the source of the arising magnetic field H and it can be expressed by Equation 3.13

$$H = cN_d M_r \theta_T \tag{3.13}$$

where c depends on the location and orientation of the field sensing device. When simplifying Equation 3.13 by substituting θ_T from Equation 3.12 the field is expressed by Equation 3.14.

$$H = \frac{c3\lambda\sigma}{\frac{2K_u}{N_d M_r} + M_r} \tag{3.14}$$

This shows the linear dependences of the arising field on the torque induced stress. The importance of choosing a material with a high λ is also obvious since it directly effects the strength of the field. For a more in depth analysis of the interrelationship between the parameters affecting the polarized ring thoroughly research has been conducted by e.g. Ivan Garshelis[15].

A circular polarized ring using one magnetic band will develop magnetic poles at the edges of the ring due to the axial component of M_r caused by torque and hence the field sensor for this configuration is located there as can be seen in Figure 2.9. A drawback for this configuration is that the orientation of the magnetization can easily be affected by an axial magnetic field since the field sensor does not differentiate between the field generated and the torque from an external axial field. A solution to this is to utilize two oppositely polarized circumferential bands [17].

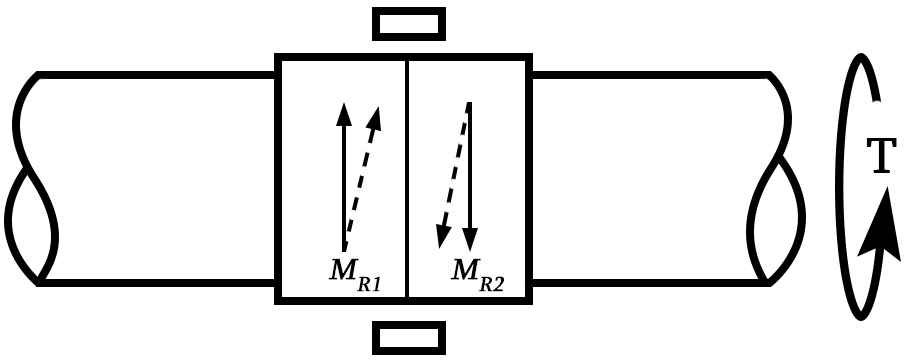

Figure 3.11: A circular polarized ring using two oppositely magnetic bands

Using the configuration seen in Figure 3.11 the two remanent magnetic fields M_{R1}, M_{R2} will rotate under applied torque. The right side of M_{R1} gives rise to the same magnetic polarization as the left side of M_{R2} creating a magnetic pole in the centre of the ring and two opposite poles at the edges of the ring. If the fields are placed in close proximity to each other the radial component of each individually generated field can be sensed by a single field sensor placed at the centre of the ring.

Adding a secondary sensor symmetrically on the opposite side of the shaft will not only give additional sensing data but the output signal of the sensor will be independent of external radial fields. Since arbitrary external fields consist of both radial and axial field components, the transducer design should be resistant to their influence to reduce the impact on the output.

The two magnetic field configuration provides by design reduced interference from external axial field. In an axial field H the two fields will regardless of circular magnetization rotate towards the direction of the external field as in Figure 3.12. The two rings having opposite polarity at the edges in the centre will not generate any detectable field for the field sensor.

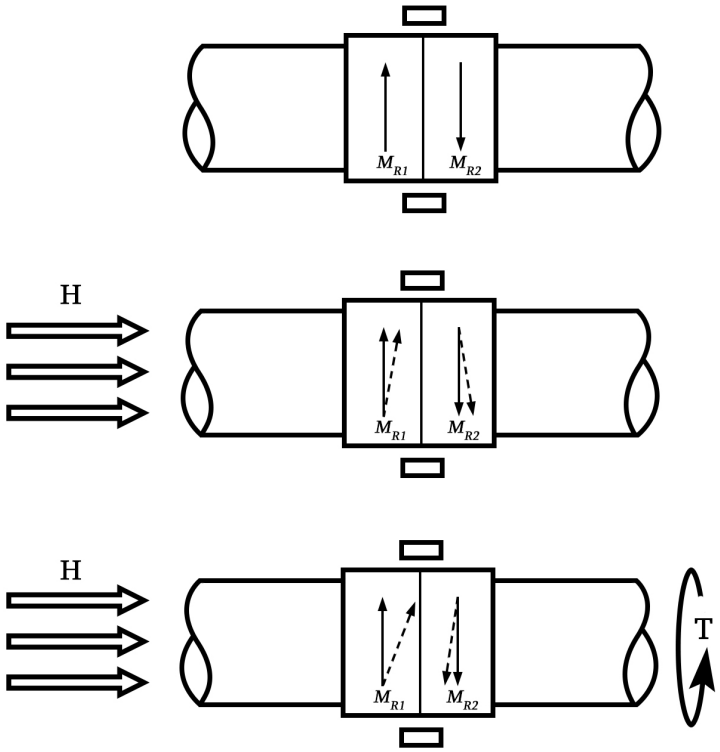

Figure 3.12: The two magnetic field configuration subjected to external axial field

When elaborating different approaches for achieving the two oppositely polarized circumferential magnetized bands one could use two separate rings each with one circular field or a single ring with two oppositely directed fields. Using two rings each with a separate field simplifies the magnetizing process as you could place the ring on a shaft and pass a strong current through it. However research have shown [16] that using a single ring with two fields provides a higher sensitivity than using two rings. In addition one ring act as a single mechanical unit during torque, improving stress transmission.

The polarized band design that was selected for further development was the single ring with two oppositely polarized circumferentially magnetized bands. This design reduces the interference from ambient magnetic field and the sensitivity is increased compared to a ring with a single circular field.

3.4.6 Ring magnetization

To create the two polarized bands, a magnetic field is tangential applied to the ring in both directions of the bands. The applied magnetic fields H must exceed the coercive force H_c of the ring to reorient its magnetization. For the concept the choice of magnetic source was using strong permanent magnets since they are more flexible than an electromagnet and fits a wider range of rings. While it is possible to use an electromagnet, there is a longer start up time to find a strong electromagnet and get the right fixture for the ring hence it is more suitable for larger scale production.

The magnets that were used were two neodymium magnet blocks of grade N35 and dimensions 25 mm X 10 mm X 5 mm. To magnetize the ring around its circumference the magnet is placed with a thin air gap from the magnet and the ring is then rotated. The circumferential distribution of the rings magnetization after one revolution can be seen in Figure 3.13.

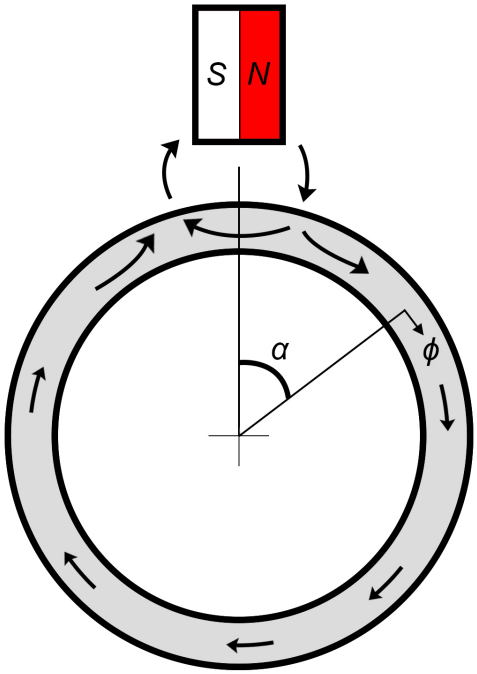

Figure 3.13: Circumferential distribution of ring magnetization after one revolution

The goal is to have a uniform magnetic orientation in the positive ϕ direction which is the rings easy axis, easiest direction of magnetization. For small values of α the magnetic field will go in the negative ϕ direction, provided that you have a small magnet compared to the ring. For slightly wider angles depending on the air gap and the ring radius, the magnetic field will change to positive [16]. If the ring is then rotated and the positive $H_{easy} > H_c$ the direction of the magnetic orientation will be in the positive ϕ direction except for a minor sector closest to the magnet after one rotation. The negative magnetization in the minor sector can be reduced and even reversed if the field from the magnet is sufficiently decreased by e.g. inserting a shield between the magnet and the ring. If the positive field from the rest of the ring acting on the minor sector exceeds H_c then whole circumference will have ha uniform positive magnetization.

The setup that was used to magnetize the ring can be seen in Figure 3.14. The two magnets were placed in close proximity to the ring with an air gap of around 0.5 mm and at a 2 mm distance from each other. The ring was then rotated about one hundred rotations and before the ring was removed from the magnets a magnetic shield was inserted between the magnets and the ring.

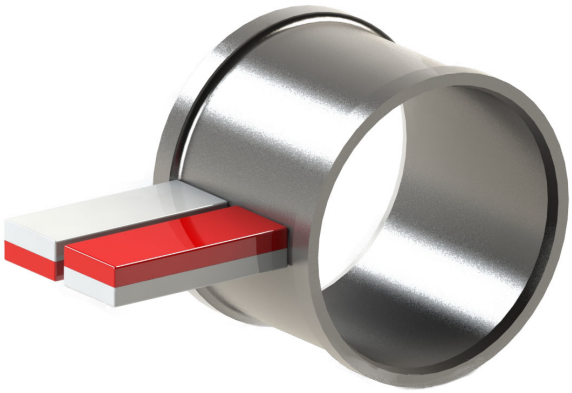

Figure 3.14: Magnetization of the ring

3.4.7 Magnetic field transducer

Price comparison

Prices of magnetic field sensors varies a lot depending on sensing technology, sensitivity, durability as well as the number of units bought. If it is a directional sensor, it could be in a one, two, or three axis configurations. Price information on retailers web pages are given for different quantities, usually a couple of thousands, but for some the price are only given for a few or only one single sensor. All these variable makes it difficult to do a quick and reliable estimation of how much the different techniques varies in price. Nevertheless a small comparison has been done. Prices have been taken from Mouser, Farnell and Digikey respective web page.

Hall sensors are by far the most commonly available sensor by a large margin, followed by AMR sensors. Only a few products using fluxgate technique have been found, but they were used for current measurement and not as a pure magnetic field sensor. Prices are taken from sensors without any extra housing or encapsulation. Prices used in this comparison are mostly given for an amount of a couple of thousands. However there are some where the price only was given for a single or few sensors.

Table 3.4 shows that the ordinary hall- and AMR sensors are in the same price range. Since the price of high sensitivity hall sensors are a lot higher than the “standard” hall sensors they were separated into two categories. The “compass” category are sensors where no information of the sensing technology was given in the datasheet. However since they are compass modules and operates in a the same range as other compasses based on AMR it is also likely they are based on the same technique.

If price information of fluxgate sensors would have been found it is likely it would have been higher than a surface mount hall or AMR sensors since they consists of both a core and a coil

Table 3.4: Price comparison

Sensor type	**Average price [Euro]**
Hall	1.58
Hall, high sensitivity (>10 mV/gauss)	15.8
AMR	1.95
Compass	0.759

and needs a driving circuit which provides an AC voltage for the driving coil and circuitry for the sensing coil. If hall sensors are going to be used it will probably have to be the one of the sensors with higher sensitivity which are ten times more expensive than the "standard" hall sensors.

In spite of the relative small number sensors used to do this comparison and the different amounts the price was given for, it shows that hall sensors are increasing rapidly in price with the sensitivity and therefore would be hard to justify using this type of sensor. The only alternative, according to this comparison is the AMR sensors which both have a lower price and a sensitivity in the range needed to sense the changes in magnetic field from the magnetoelastic material.

3.5 Creating prototype

3.5.1 Sensor element and shaft

The magnetoelastic ring was made according to the parameters calculated in chapter 3.4.3. Rings were pressed on two different shafts to preform tests on. Both shafts were slightly lathed just to get finer tolerances to achieve the calculated contact pressure. On one shaft a groove was made to half the diameter to make it weaker and less torsionally rigid and more prone to twist when torque is applied. The rings were then welded at the sides to make them rigidly attached to the shaft to avoid any slip.

Figure 3.15: Left: weakened shaft, middle: shaft with pressed on ring, right: weakened shaft with welded ring

3.5.2 Electronics

To collect the data from the sensor it was connected to an Arduino due microcontroller based on an 32 bit ARM cortex-M3 CPU running at 84 MHz which should give plenty power to collect and process the sensor data. The first sensor, left in Figure 3.16, consisted of one HMC5883L 3-axis magnetometer and it communicates via an I2C bus. The operating range can be changed from ± 0.88 to ± 8 gauss. Because the magnetization did not give a completely homogeneous magnetic field it affected the readout negatively. This single sensor arrangement was replaced by four magnetometers, to the right in 3.16, of the same kind but glued together side by side at an angle to embrace the shaft.

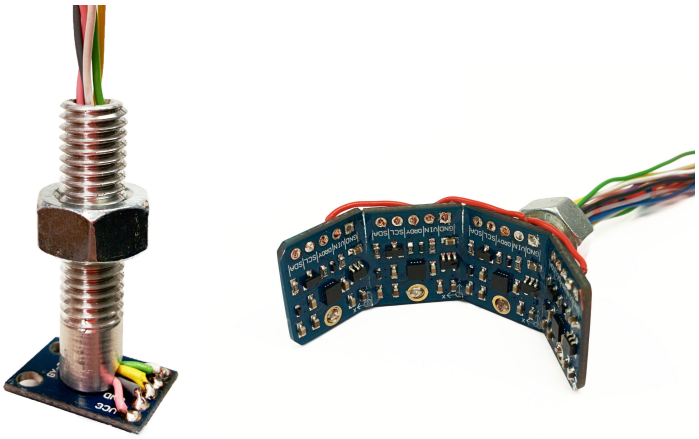

Figure 3.16: The two magnetic field sensors used

This made it possible to get sensor data from four different places on the shaft at the same time and then combining it to get an average which is not fluctuating as much as the data from each individual magnetometer. To further suppress spikes a simple low pass filter was implemented. To be able to mount it in the coupling and get the 14 cables out the housing an aluminium tube was attached to the back of the sensors.

The sensors has a maximum data output rate of 160 samples per second. Since all three axis from each sensor was printed both filtered and unfiltered this speed was not reached with the serial communication and a maximum baud rate of 115200. The output rates of about 50 Hz that was achieved is enough to measure torque changes for low RPM. In Figure 3.17 the Gen V coupling is fitted with the sensor prototype. The magnetic field sensor is attached trough a hole in the housing right above the sensor element.

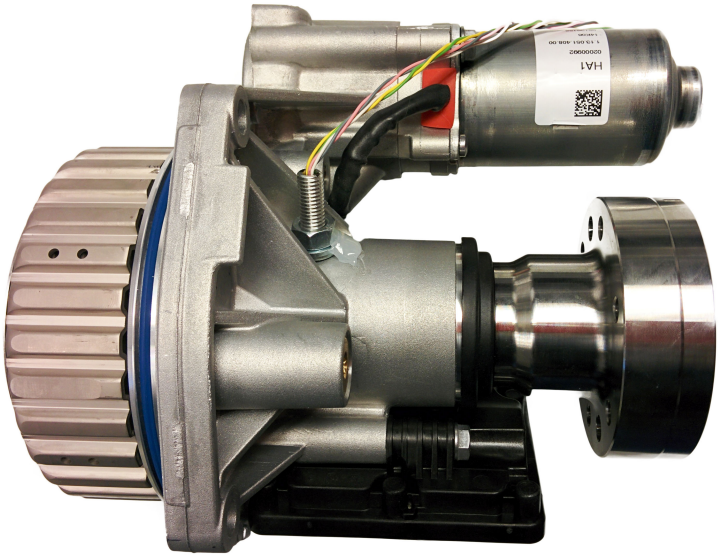

Figure 3.17: The Gen V coupling is fitted with the sensor prototype

4

Testing

To test and verify the performance of the sensor prototype tests will be made on the ring itself and in test rig when it is mounted on the shaft inside the coupling. The tests on just the ring itself will be made to know how the magnetoelastic material behaves when mechanical stresses are applied, without having the shaft interfering with the result. When the rings are fitted onto the shaft the tests will give results of how it all preforms together as in a real application.

Tests will be done where the torque is ramped up and down, as well as stepped up and down.

4.1 Method

The test rig used to test the sensor when it is mounted inside the coupling rotates the shaft with up to 50 revolutions per minute. To apply torque, a brake is engaged which prevents the outgoing shaft to rotate. The difference in rotational speed is possible due to the fact that the lamellas are sliding in relation to each other. To control the torque, the oil pump in the coupling is driven at different speeds which causes the piston to compress the lamella package and torque is transferred to the shaft. It is not the setpoint given to the ECU that is used as reference for the measurements. The reference is provided by a strain gauge in the rig. The sensor's Z-axis was always pointing in the radial direction. The X- and Y-axes are pointing in the circumferential and axial direction as in Figure 4.1.

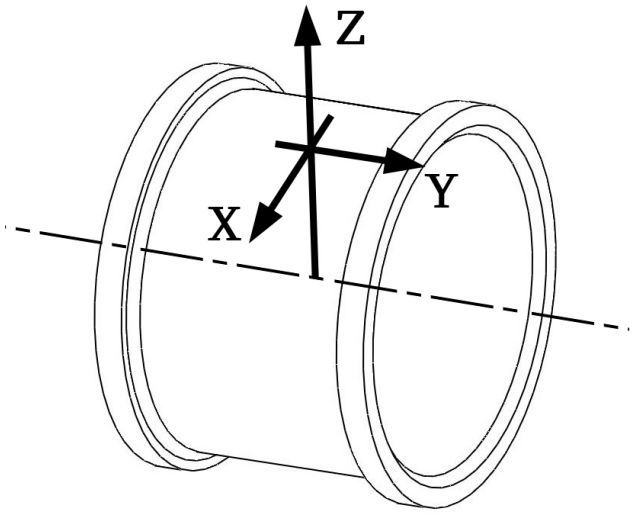

Figure 4.1: Position of the magnetometer axes in relation to the sensor element

4.2 Initial tests

Before the sensor and ring were mounted in the coupling and tested in a rig, some initial tests were conducted on the individual parts. To determine how the magnetic field changes in the magnetic ring when it has been press-fitted on the shaft and experiences a lot of circumferential and axial stresses, a test was done with the sensor mounted inside the coupling by just rotating the shaft with no load. The tests showed variations in magnetic field around the circumference of the ring, Figure 4.2. To reduce these changes different ways of magnetizing the sensing element were tested. The results were compared to see which configuration gave the smallest changes in magnetic field around the circumference of the ring.

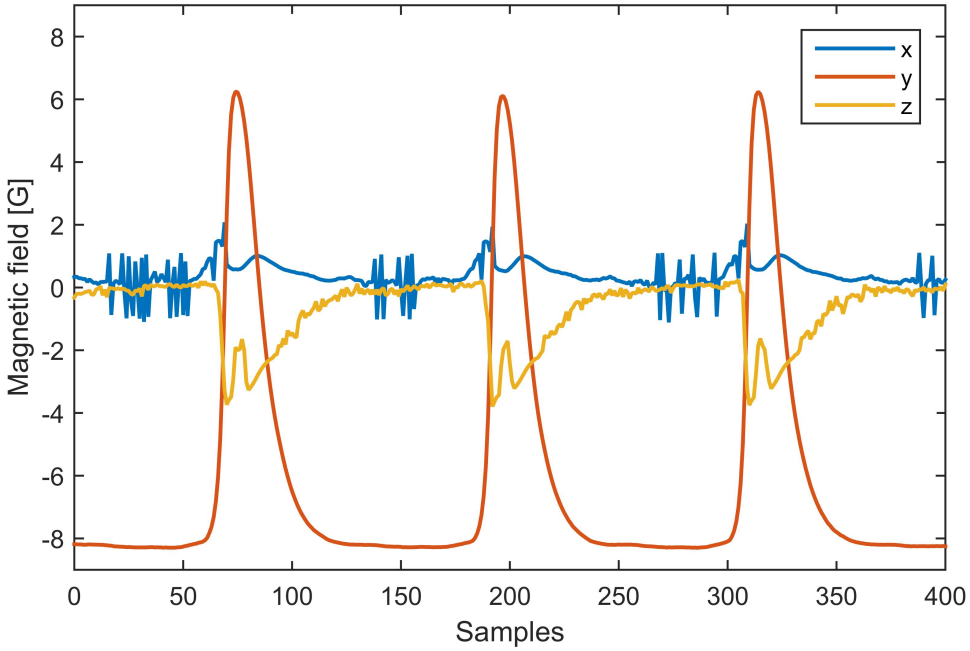

Figure 4.2: Magnetic field from unloaded shaft

Since the shaft itself is ferromagnetic and thus could interfere with the magnetometer, tests were done with no ring mounted to the shaft, Figure 4.3. It shows a change of the magnetic field of about 4 gauss with the sensor pressed against the shaft. When the rings are mounted and the sensor is placed with a thin air gap from the magnetic ring the field from the shaft will be reduced considerably.

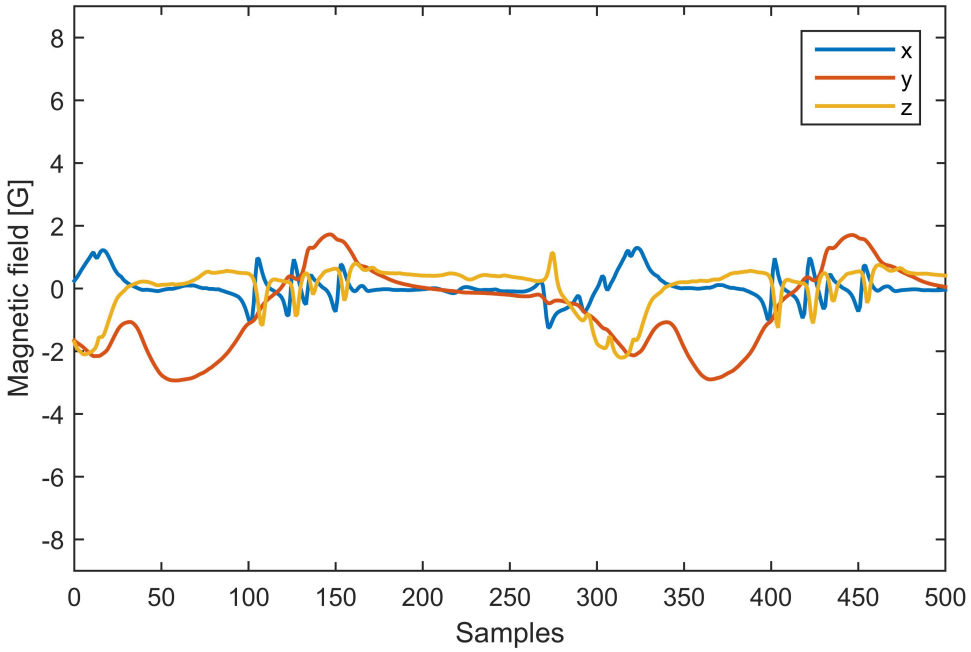

Figure 4.3: Magnetic field produced by the shaft

As described in chapter 3.4.6, the magnets were placed directly against the ring while it was rotated according to Figure 3.14. However, wide spikes with large amplitude occurring once per revolution where the magnets had been removed were still present. The width of the spikes were reduced by stopping the rotation of the shaft before removing the magnets, Figure 4.4.

To reduce the amplitude, a shield made of both magnetic steel and non-magnetic brass was constructed. It was placed between the rings and the magnets during magnetization. The non-magnetic brass was supposed to not interfere with the magnetic field from the magnets. When the magnetization procedure was done the ferromagnetic steel part was pulled in between the ring and the magnet and thus reducing the field experienced by the ring. The magnets was then pulled away. The result of this is seen in Figure 4.5.

The number of revolutions the ring was turned during magnetization was increased approximately 3 times to about 100 revolutions. This further decreased the variation in magnetic field. The Z-axis now only have one peak of about 3 gauss per revolution and a variation of less than a gauss between the peaks Figure 4.6.

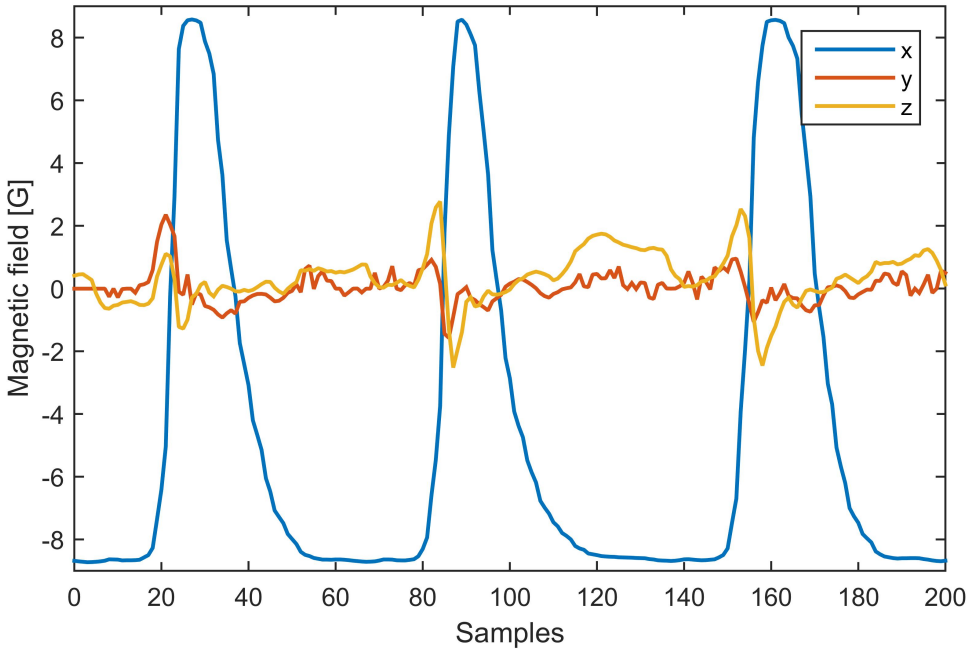

Figure 4.4: Rotation stopped before the magnets were pulled away

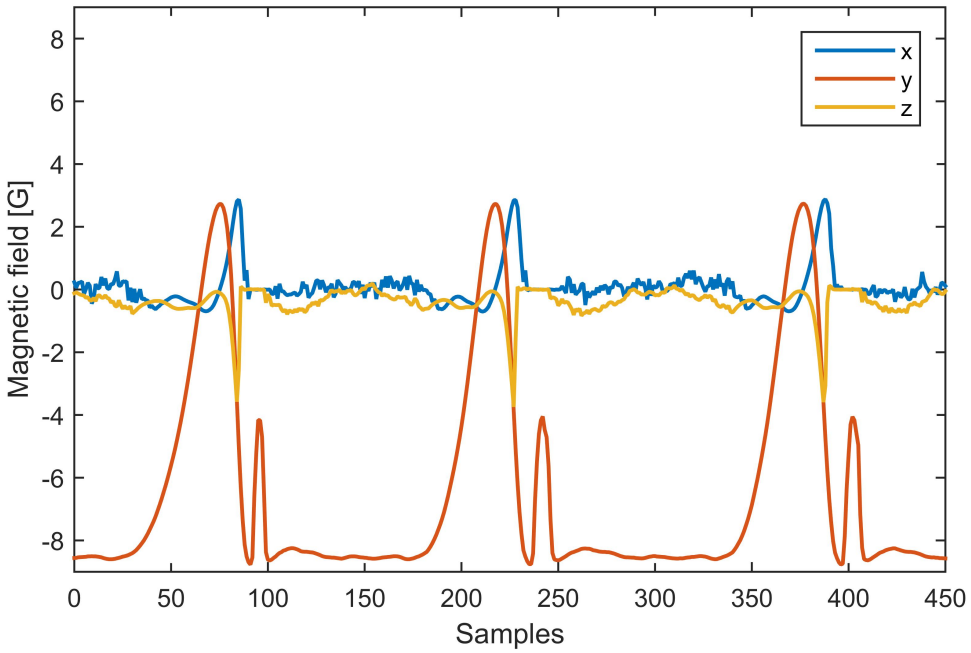

Figure 4.6: Long magnetization

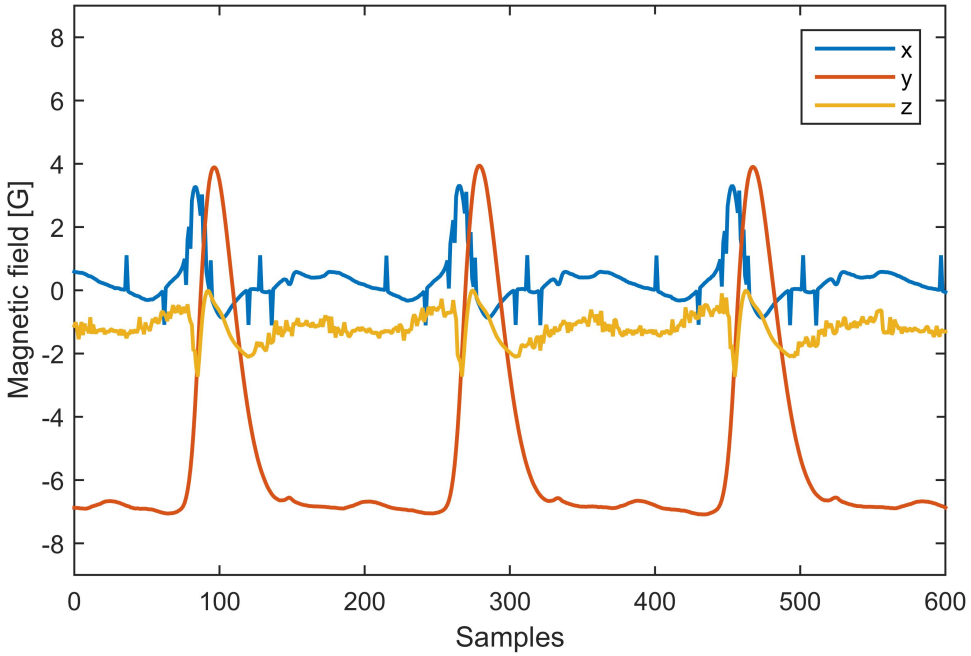

Figure 4.5: Magnetized with shield

4.2.1 Static torque tests

To test the magnetoelastic effect before the ring is pressed on the shaft, some static torque tests were performed. The ring was rigidly attached in one end with a clamp to a fixture and the other end was attached to a rod. The rod was then manually twisted to apply the torque on the ring. A magnetometer was glued to the side of the ring. The fixed position of the magnetometer in relation to the ring neglects the effect of the the uneven magnetization. It was possible to apply a torque of a couple of tens of newton meter before the clamp started to slide. A scale was used to measure the force pulled on the rod and with a known length of the lever the torque was calculated. The Figure 4.7 shows the result of a test where torque was applied increasingly with from 0 to 11 Nm in about 0,7 Nm increments. The sensor values were read manually from the data stream when the desired force was reached.

The accuracy is therefore not very high, but it gives a good indication of the magnetoelastic behavior of the ring. The force was only applied on one end of the rod which gives stresses in directions other than only torque. The fastening of the rod to the clamp caused some radial compression if the ring when torque was applied which also contributed to stresses in directions other than what is caused by torque. To test the hysteresis of the magnetoelasticity, an alternating positive and negative torque was applied on the ring, seen in Figure 4.8.

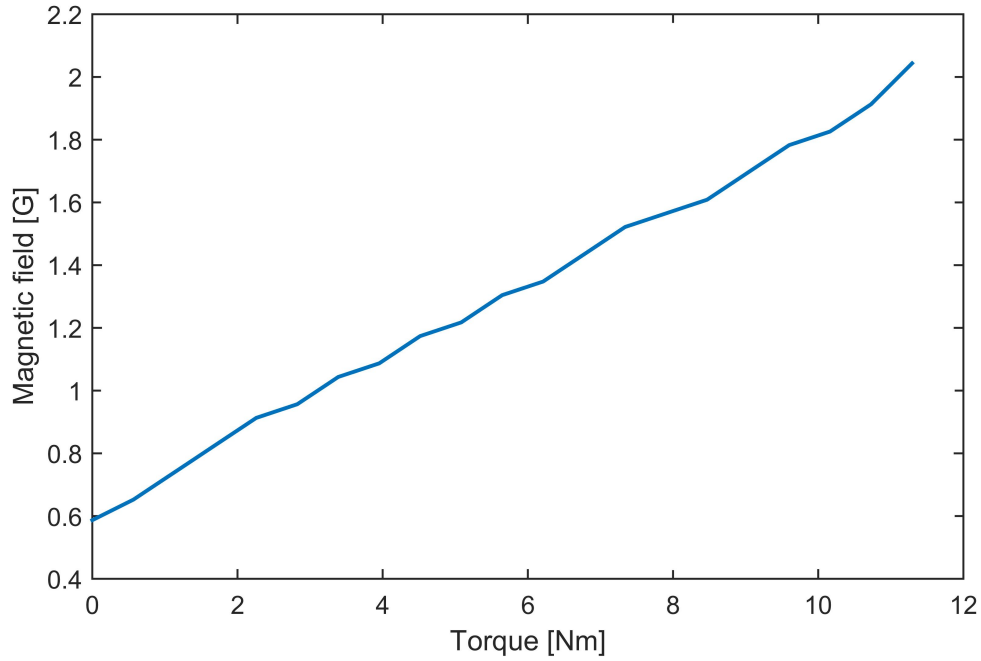

Figure 4.7: Static torque test of the ring

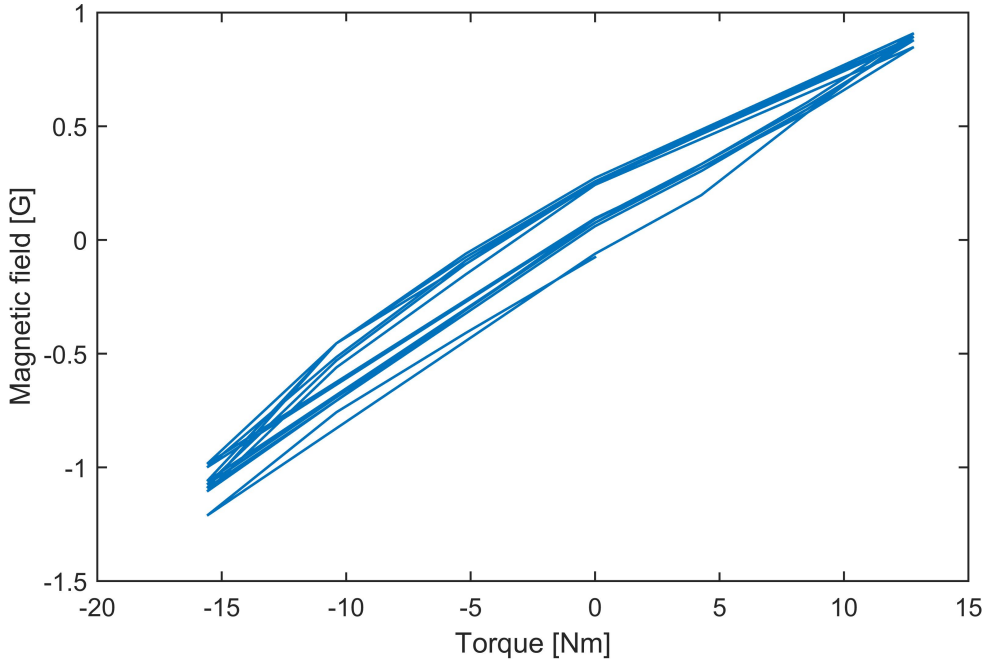

Figure 4.8: Hysteresis

4.3 Tests in coupling

The tests of the sensor prototype when it was mounted inside the coupling were done in a test rig. The rig is able to apply a torque of 2000 Nm on the coupling with rotation in both directions. The torque is controlled just like in a car with the couplings internal oil pump. The output shaft can be either be unlocked, i.e. the shafts spins freely and no torque is transferred, or locked i.e. the output shaft is stationary and torque is transferred. The brake is operated with an electromagnet which interferes to some degree with the magnetometer but not enough to saturate it.

The figures with only one magnetometer axis and a reference should not be compared with each other with regards to the amplitude since they are scaled to fit the reference. This comparison can be made in Figure 4.16, 4.20 and 4.24 where all three axes are plotted in the same graph.

4.3.1 Pressed on ring

This test consists of a ramp up to 900 Nm where the brake is released for a short time and then re-engaged to ramp the torque down to 0 Nm again. This is shown as the orange line, denoted "ref", in all figures from the rig tests. The results from the three axes are seen in Figure 4.9 to 4.12. The goal was to get the magnetic field strength to change.

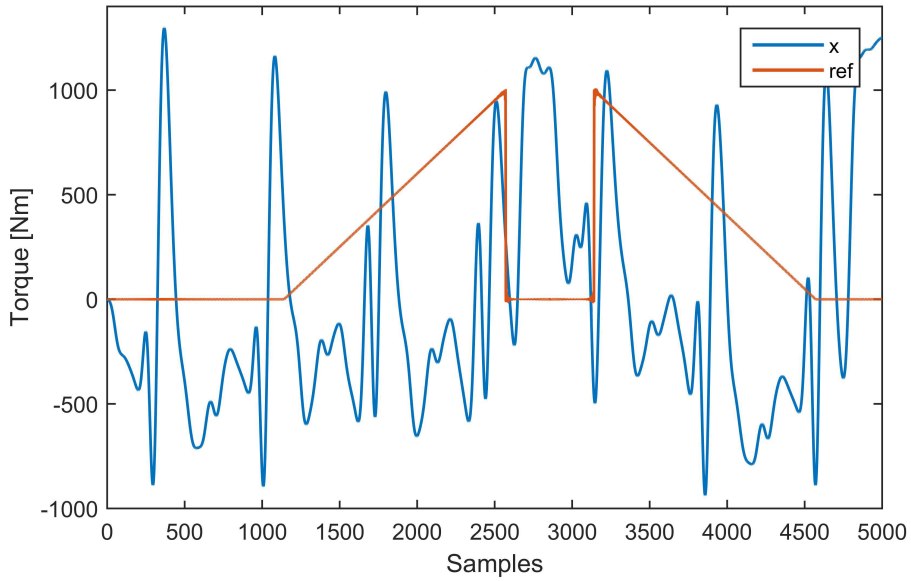

Figure 4.9: Magnetic field, tangential direction

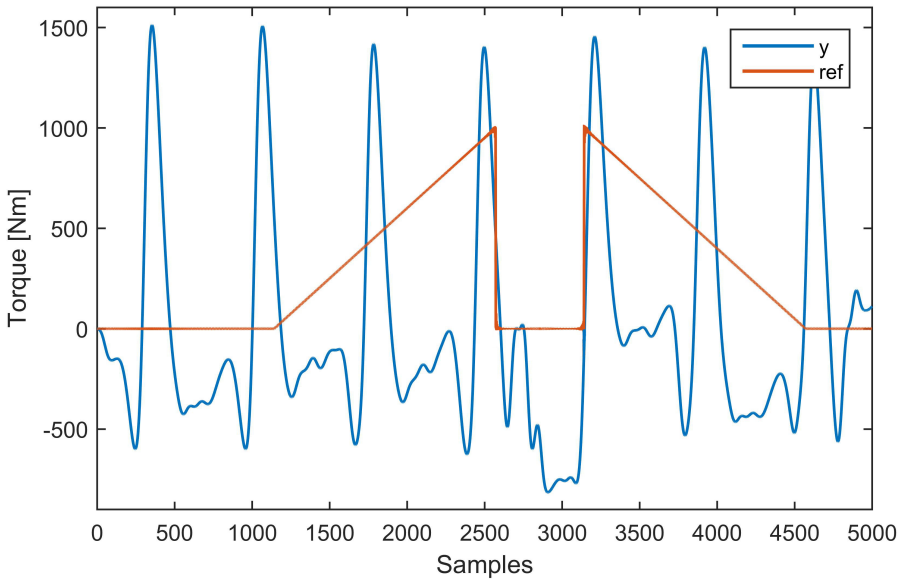

Figure 4.10: Magnetic field, circumferential direction

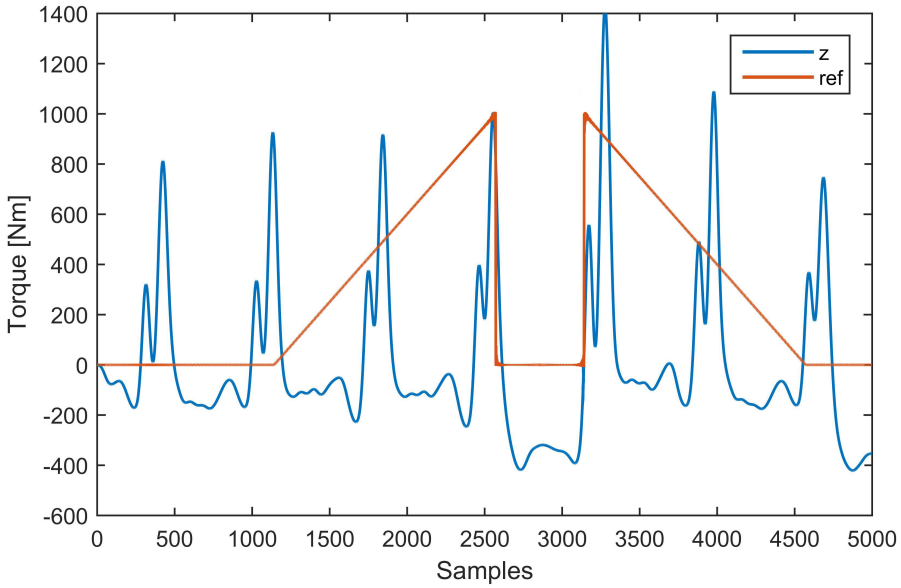

Figure 4.11: Magnetic field, radial direction

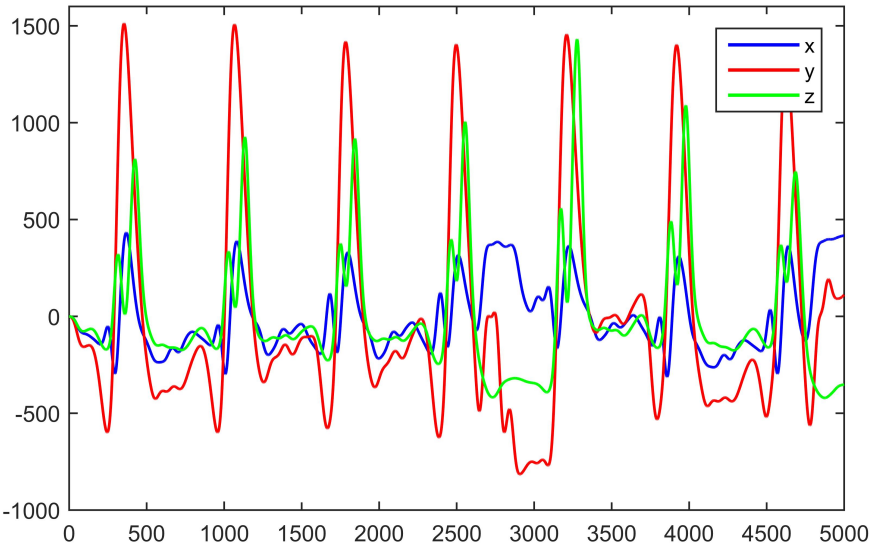

Figure 4.12: All three directions

4.3.2 Welded ring

In the first test the torque is increased to 250 Nm in two steps and then back to 0 Nm. This was repeated three times. Fig 4.13 ,4.14 and 4.15 shows plots from the x, y and z axis of the magnetometer. Table 4.1, 4.2 and 4.3 roughly shows the change in magnetic field due to the torque, how many sensor increments it corresponds to at the lowest sensitivity of the sensor, used during the test, as well as for the highest sensitivity. The field Nm/counts shows how many Nm each sensor count corresponds to.

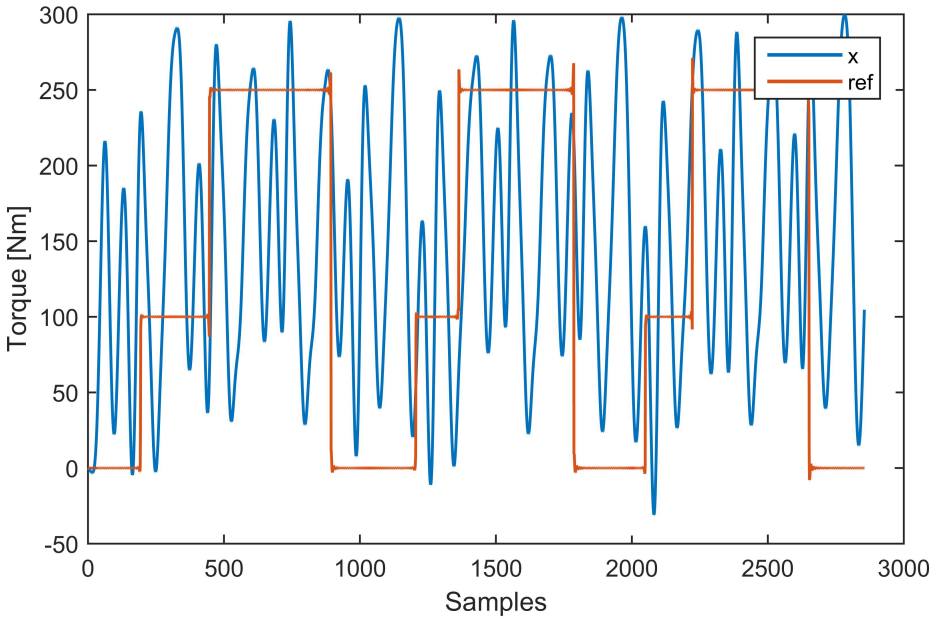

Figure 4.13: Magnetic field, tangential direction

Table 4.1: Change in magnetic field

Axis	Change [mG]	Counts (4.35 mG/LSB)	Nm/Count	Count(0.73 mG/LSB)
X	45	10	25	60
Y	330	76	3.3	450
Z	410	94	2.7	560

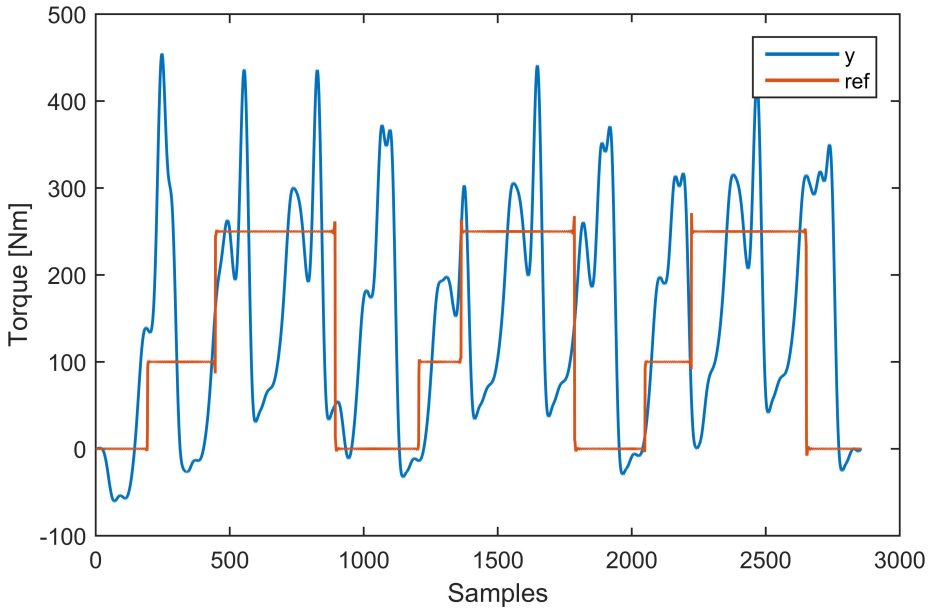

Figure 4.14: Magnetic field, axial direction

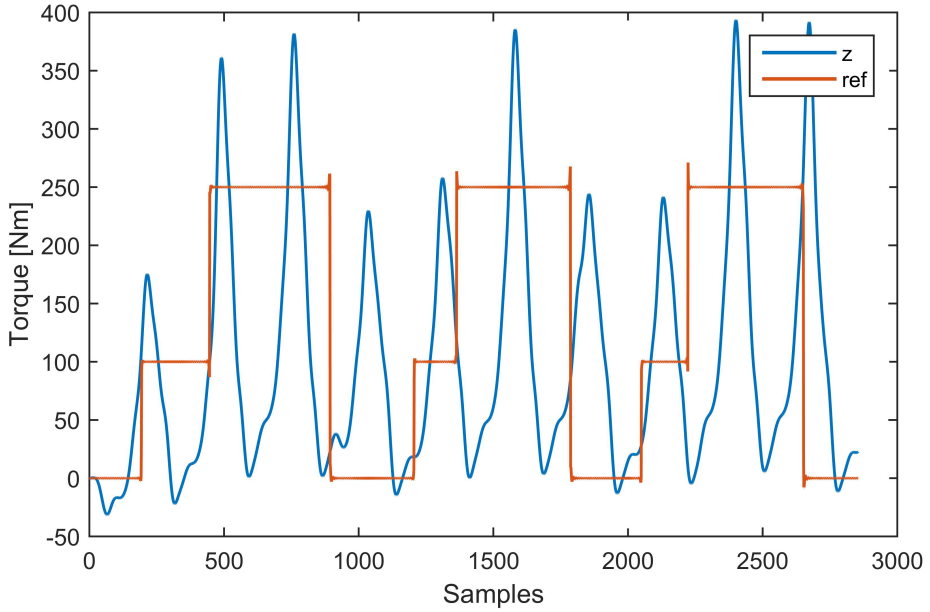

Figure 4.15: Magnetic field, radial direction

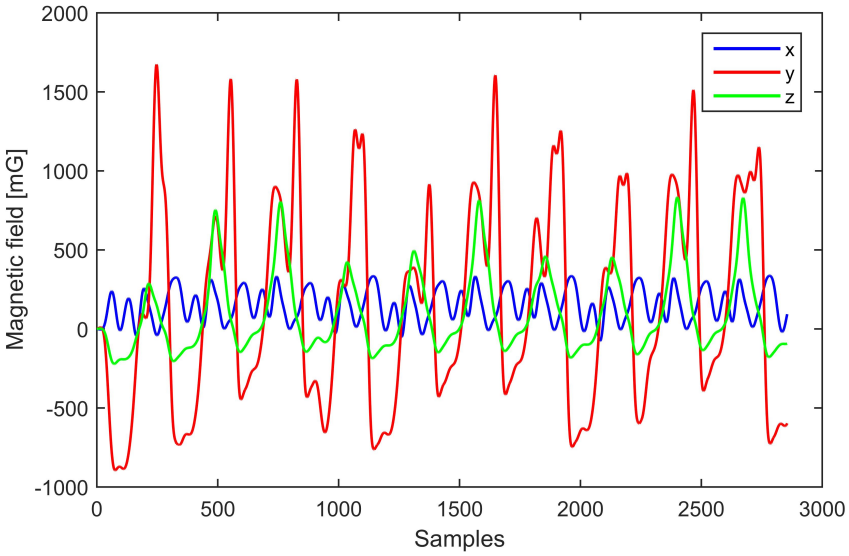

Figure 4.16: All three directions

In the second test the torque was also increased to 250 Nm but in steps of 50 Nm. Figure 4.17, 4.18 and 4.19 shows the result of this test.

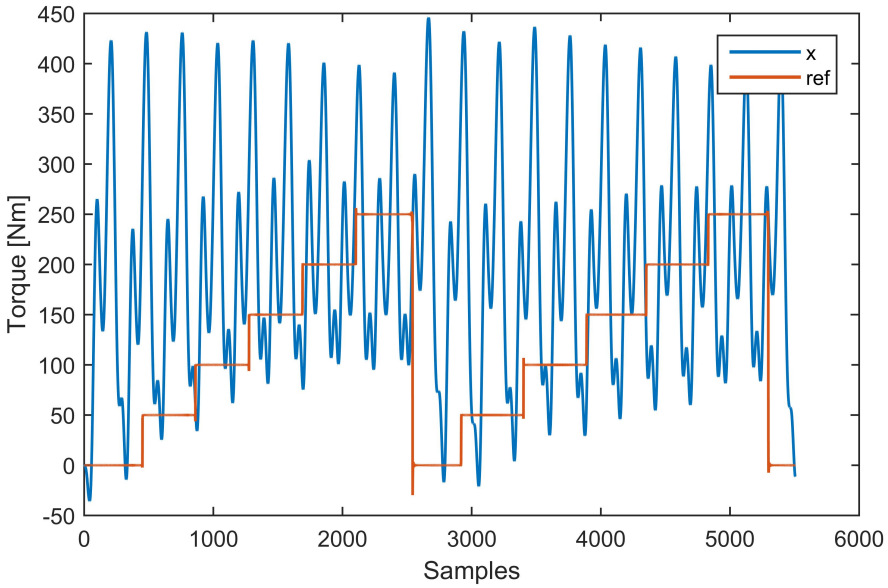

Figure 4.17: Magnetic field, tangential direction

Table 4.2: Change in magnetic field

Axis	Change [mG]	Counts (4.35 mG/LSB)	Nm/Count	Count(0.73 mG/LSB)
X	80	18	14	110
Y	540	120	2	710
Z	440	100	2.5	600

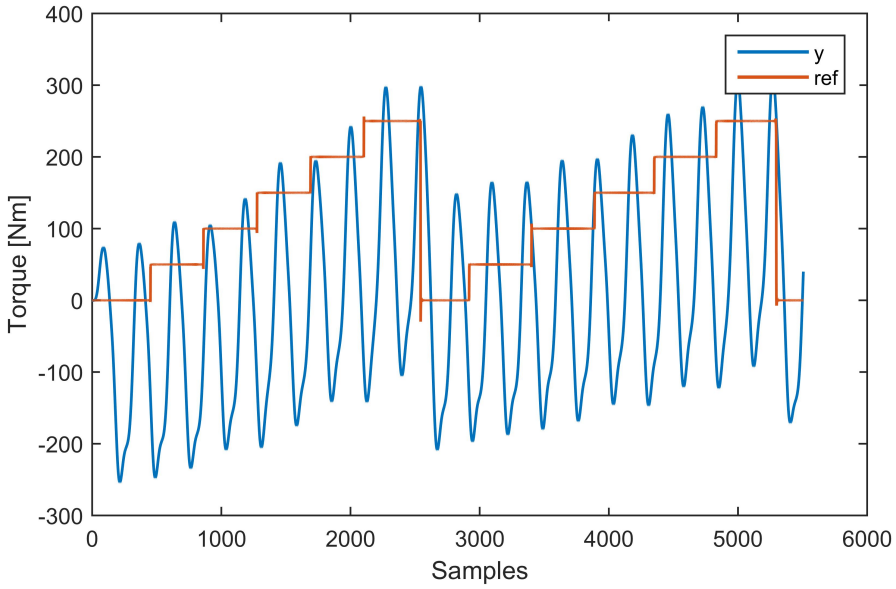

Figure 4.18: Magnetic field, axial direction

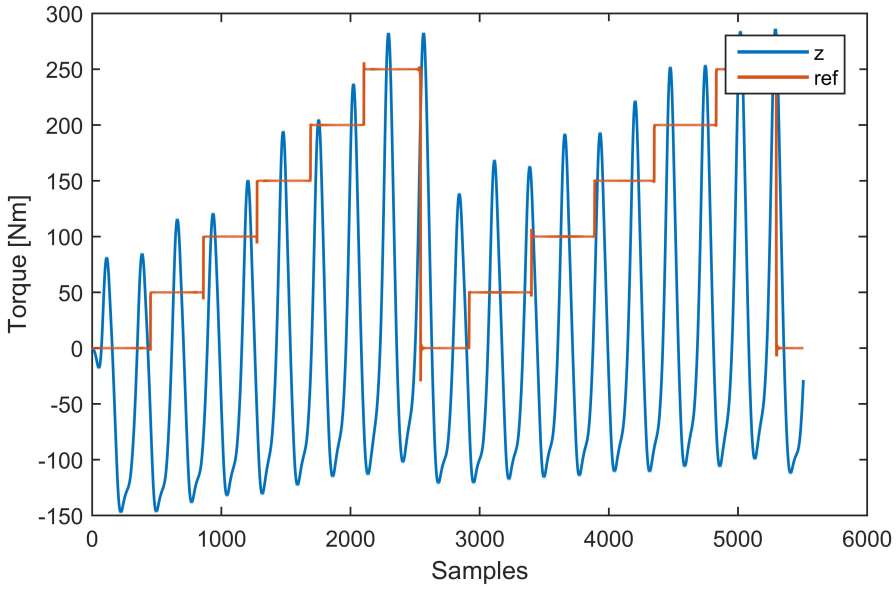

Figure 4.19: Magnetic field, radial direction

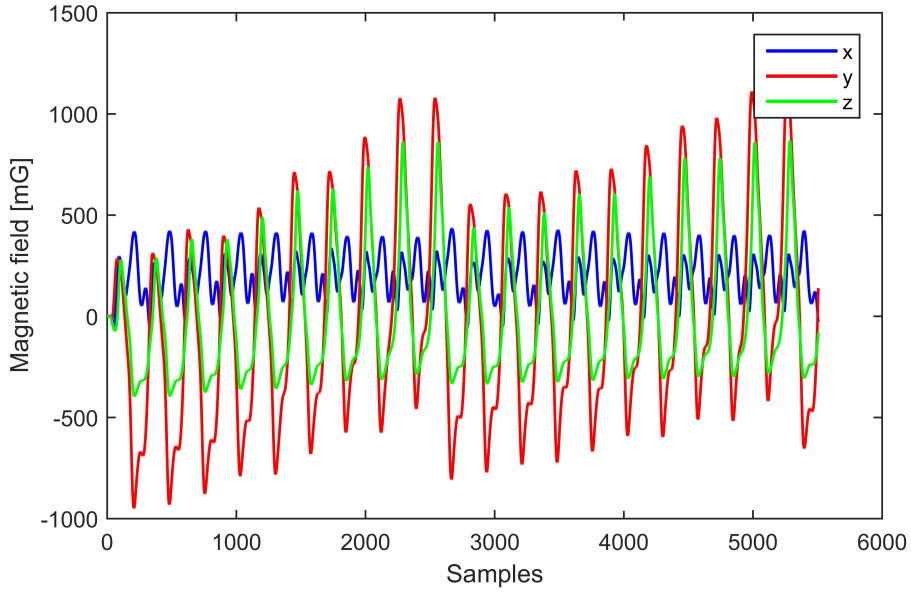

Figure 4.20: All three directions

The third test was alternating between ±250 Nm to test the hysteretic properties. Figure 4.21, 4.22 and 4.23 show the result of this test

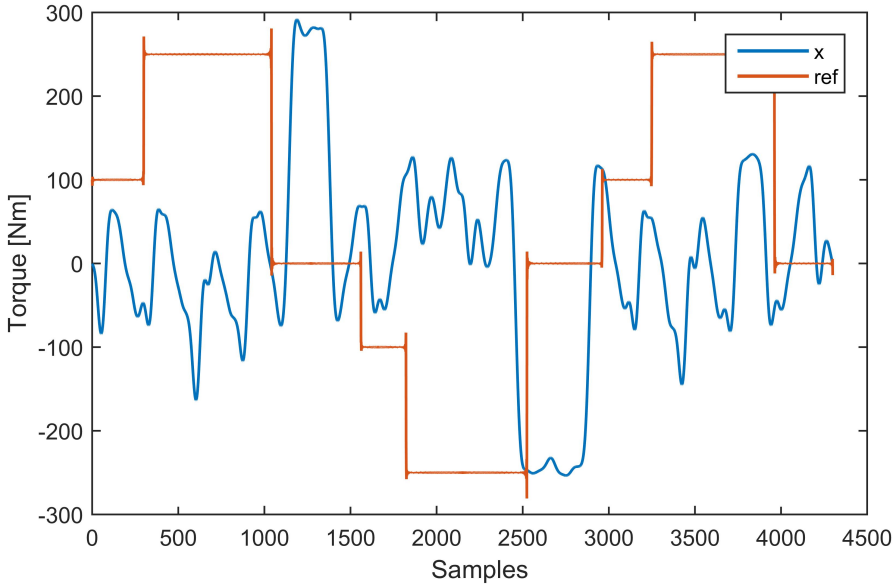

Figure 4.21: Magnetic field, tangential direction

Table 4.3: Change in magnetic field

Axis	Change [mG]	Counts (4.35 mG/LSB)	Nm/Count	Count(0.73 mG/LSB)
X	230	52	10	310
Y	460	110	4.5	660
Z	210	49	10	290

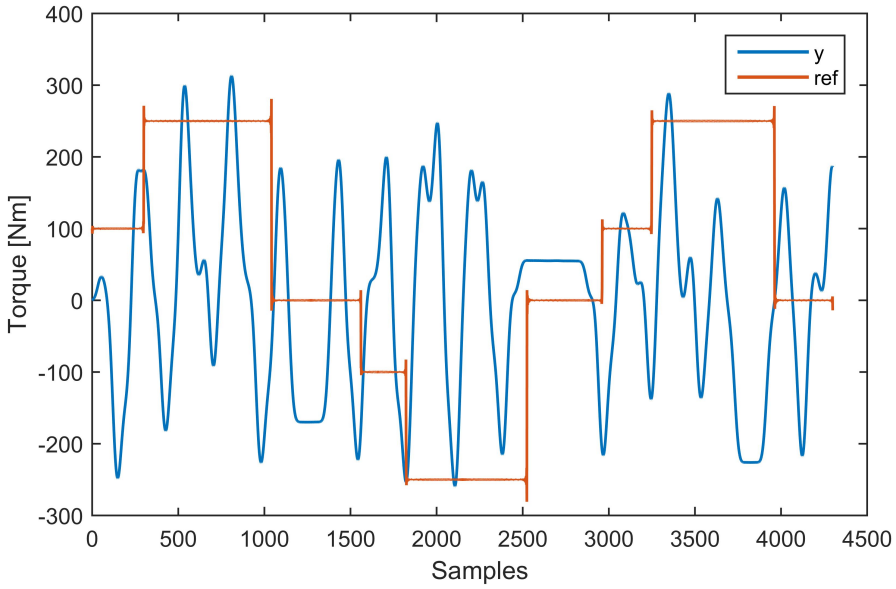

Figure 4.22: Magnetic field, axial direction

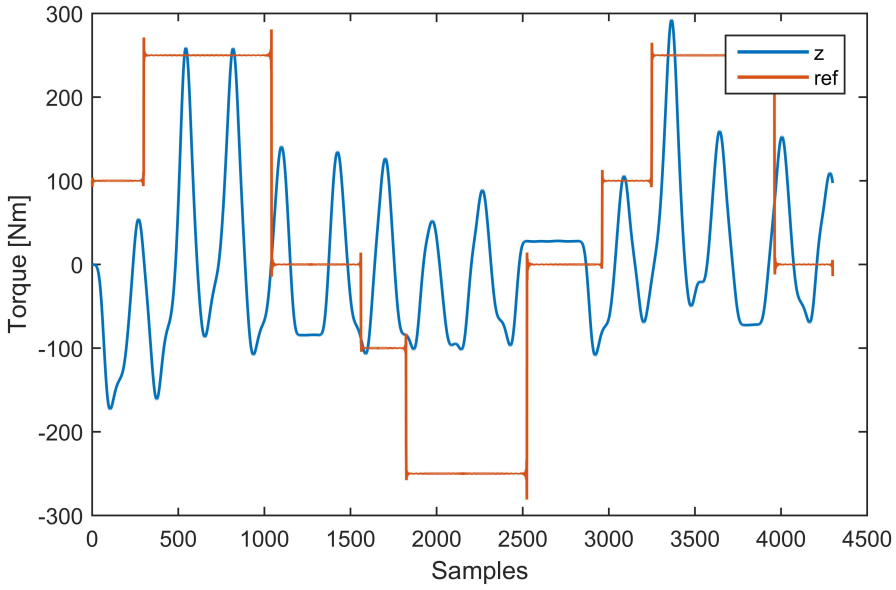

Figure 4.23: Magnetic field, radial direction

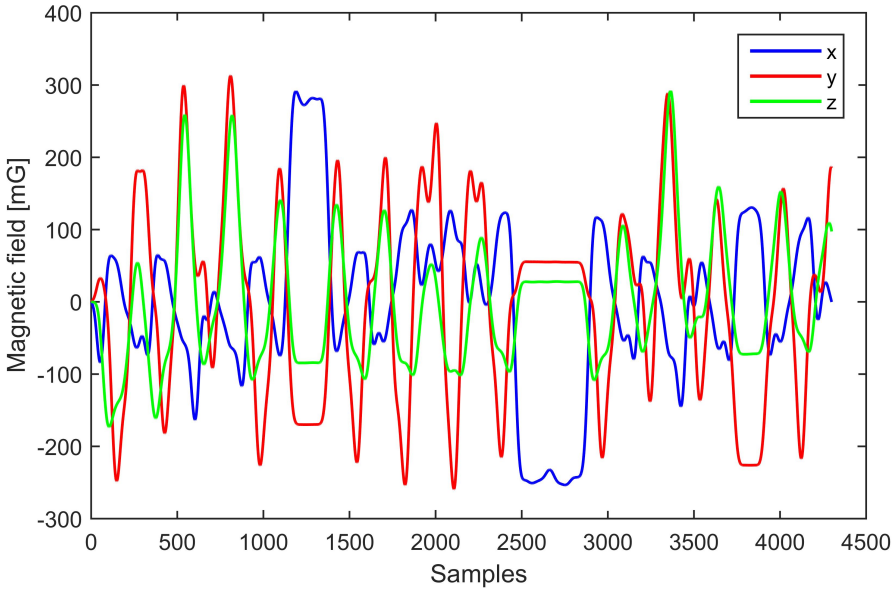

Figure 4.24: All three directions

5

Analysis

5.1 Initial tests

The initial test shows the unevenness of the magnetization of the ring. The magnetic variations were partially decreased by magnetizing for a longer period as well as using a shield. The shield is supposed to reduce the field experienced by the ring when the magnets were pulled away, and thereby not change the remanent field in the ring.

The torque test showed a relatively linear relationship between torque and magnetic field. Since this test was done with the magnetometer glued to the ring the of the circumferential variations did not affect the plot, but when changing the position the response to applied torque changed. These changes are probably partly a result of the uneven magnetization. However, the arrangement with the clamp and lever deformed the ring into an elliptical shape when force was applied. The stresses arising in the ring during this deformation will not be the same as for pure torque, hence this test gives information what happens when stress is applied and not just torque.

The result of alternating between positive and negative torque shows some hysteresis. The deviation around $x = 0$ is approximately 0.2 gauss and the total change is almost 2 gauss. Since the force was applied by hand the test is not totally accurate but gives an indication of how much hysteresis the magnetoelastic material produces.

5.2 Tests in rig

5.2.1 Pressed on ring

The test with the shaft, where only the rings were pressed on did not produce satisfying results. When the torque of 900 Nm was applied some change was seen but not enough to get any useful data. The lack of response is probably caused on the isolating ring with its 2 mm wall thickness. It prevented stresses to be transferred to the magnetoelastic ring. A trade-off has to be made on a separation distance between the shaft and the magnetoelastic ring to prevent magnetic flux leaking into the shaft and the increased torsional rigidity the ring provides. The magnetoelastic ring can also be made thinner, but how much this will affect the strength of the magnetic field have to be investigated further.

5.2.2 Welded ring

As in the initial test the circumferential changes of the magnetic field are the dominating variations. Torque induced variations are still clearly visible in some of the tests. In the two first tests the Y- and Z-axis shows considerably larger changes compared to the X-axis when torque is applied. This is not the case with the hysteresis test where the response from the X-axis is comparable to the Z-axis.

The best result is given by the second test where the torque has been increased in steps of 50 Nm. Some hysteresis can be seen when the torque is brought back to zero but the sensor value does not return to the last zero value.

In Figure 4.19 the valleys does not respond to the torque as much as the peaks. This could mean that it is both the direction of the magnetic field as well as the strength of it that are changing around the circumference. This could imply the magnetic field during the magnetization was not strong enough to change the direction of the magnetic dipoles of the ring.

The greatest change in magnetic field, due to torque, was produced by the y-axis in test 2, 540 mG Table 4.2. This is about the same magnitude as earth's magnetic field which could cause problem when it is interfering with the sensor. However Figure 4.7 in chapter 4.2.1 shows that the magnetic field change almost one gauss without saturation. A greater change in magnetic field would thereby be possible if the ring is subjected to more tension.

6

Discussion

After comparing the different methods for measuring torque in the coupling and analysing the results from the tests, the Polarized band sensor looks like a promising technique. At the current state of the prototype it is clear that more work is needed to improve its reliability and accuracy. However the simplicity of the technique along with its compact size makes it fit for integration in the coupling and suited for high volume production. The results, especially from Figure 4.19 shows a clear relationship between the applied torque and the signal.

All tests in the rig are stationary. Possible external magnetic fields will thereby only give stationary errors. In a real application the vehicle is moving and will be subjected to varying external fields e.g. the earth's. How the sensor is going to respond to this is not known and have to be further investigated. Solutions of this problem could be shielding of the sensor to prevent external fields from reaching the sensor. To shield magnetic fields can however be hard. An alternative solution could be to compare two axes that respond in a synchronized manner to the applied torque such as the y- and z-axis in Figure 4.20. If only one of them changes it would be an indication of an external field rather than a change from torque. If the direction of the vehicle is given from other sensors, their data could be used to compensate as well.

The variations in magnetic field around the circumference of the ring makes it hard to get good readouts. Different methods of magnetizing the ring can be tested to get a more homogeneous magnetization. The variations could also be an effect of using a too weak magnetic field when magnetizing and thus not change the magnetic domains as intended. To get a stronger magnetic field an electromagnet could be used instead of a permanent magnet.

As seen in Figure 4.19 the amplitude increases with the torque. An alternative to suppress the spikes would be to use their amplitude as a measure of the torque. By adding several spikes around the circumference a higher update frequency, compared to one per revolution, will be possible. With the current sampling data, the low pass filter needs to use values from several revolutions back in the time to get a signal without the spikes. Adding more spikes will allow for better filtration of the signal and faster response.

The pressed on rings did not give satisfying results because of their torsional rigidity which prevented the rings to twist together with the shaft. A retaining compound which glues the shaft and rings together could be used to improve the torque transfer ability of the frictional bond. In combination with thinner rings, larger stresses will arise and produce a greater magnetic field.

The sensor resolution is dependent of multiple factors. The magnetometer gives an output change, at its most sensitive setting $\pm$ 0.88 Gauss, of 540 increments. In the coupling used during testing it corresponds to an accuracy of approximately 2 Nm. What is more likely to limit the resolution is how accurate the magnetometer values are interpreted and how well the hysteresis can be attenuated. The effect of hysteresis could be compensated by e.g. use Preisach modelling,

which is a well known method and specially accurate for ferromagnetism.

If only the peaks, Figure 4.18 are used as a measure of the torque the update frequency will be limited by the number of peaks. If the angular position of the shaft is tracked with e.g. a lookup table where the variations of the magnetic field are sampled for a complete rotation, the measured values could be compared to the stored values. The difference between these two values will give the torque.

Finally, since the sensor should be an integrated part of the coupling, it affects the design of the rest of the coupling e.g. the ECU and the housing. This means that if the sensor is implemented it requires an overview of the whole design. Given more freedom to design the sensor the solution could be further optimized for high volume production.

Bibliography

[1] *A beginners guide to accelerometers*. URL: http://www.dimensionengineering.com/info/accelerometers (visited on 11/10/2014).

[2] Mazhar Ali et al. *Large, non-saturating magnetoresistance in WTe2t*. Tech. rep. 2014.

[3] Richard Boll and Kenneth J. Overshott. *Sensors, A Comprehensive Survey, Magnetic Sesors*. Vol. 5. Willey-VCH, 1989.

[4] Bosch. *Study TSS*. 2014. URL: http://www.bosch-presse.de/presseforum/details.htm?txtID=4332&tk_id=108.

[5] *Capacitive Linear Displacement Sensors An Overview*. URL: http://www.lionprecision.com/capacitive-sensors/index.html#apps (visited on 11/10/2014).

[6] Cogne. *IMCO420A - 1.4021*. 2015. URL: http://www.cogne.com/schedeprodotti/bars/grade/IMCO420A.pdf (visited on 04/21/2015).

[7] Orvar Dahle. "Torque Transducer". Pat. US 4135391. 1979.

[8] Gunnar Dahlvig. *Konstruktionselement och Maskinbyggnad*. Liber, 1999.

[9] Frachon Didier, Gérald Masson, and Didier Angleviel. *Development of a Contactless Hall effect torque sensor for Electric Power Steering*. Tech. rep. 2005.

[10] *Eddy-Current Sensors Overview*. 2013. URL: http://www.ni.com/white-paper/10291/en/ (visited on 04/02/2015).

[11] William. J Fleming. *Magnetostrictive Torque Sensors - Comparison of Branch, Cross, and Solenoidal Designs*. Tech. rep. 900264. SAE International, 1990.

[12] *Friction and Coefficients of Friction*. URL: http://www.engineeringtoolbox.com/friction-coefficients-d_778.html (visited on 05/10/2015).

[13] Ivan J. Garshelis. "A Study of the Inverse Wiedemann Effect on Circular Remanence". In: *IEEE Transactions on Magnetics*. Vol. Mag-10. IEEE International, 1974.

[14] Ivan J. Garshelis. "A Torque Transducer Utilizing A Circularly Polarized ring". In: *IEEE Transactions on Magnetics*. Vol. 28. IEEE International, 1992.

[15] Ivan J. Garshelis. "Investigations of Parameters Affecting the Performance of Polarized Ring Torque Transducers". In: *IEEE Transactions on Magnetics*. Vol. 29. IEEE International, 1993.

[16] Ivan J. Garshelis and Christopher R. Conto. “A magnetoelastic torque transducer utilizing a ring divided into two oppositely polarized circumferential regions”. In: *Journal of Applied Physics* (1996).

[17] Ivan J. Garshelis and Christopher R. Conto. “A Torque Transducer Utilizing Two Oppositely Polarized Rings”. In: *IEEE Transactions on Magnetics*. Vol. 30. IEEE International, 1994.

[18] Ivan J. Garshelis et al. *Development of a Magnetoelastic Torque Transducer for Automotive Transmission Applications*. Tech. rep. 970605. SAE International, 1997.

[19] Ivan J. Garshelis et al. “Magnetostriction and Magnetization of Common High Strength Steels”. In: *IEEE Transactions on Magnetics*. Vol. 40. IEEE International, 2009.

[20] *Hall Effect Sensing and Application*. URL: http://sensing.honeywell.com/index.php?ci_id=47847.

[21] *How a Fluxgate Works*. 2015. URL: http://www3.imperial.ac.uk/spat/research/areas/space_magnetometer_laboratory/spaceinstrumentationresearch/magnetometers/fluxgatemagnetometers/howafluxgateworks (visited on 04/02/2015).

[22] Brian D. Kilmartin. *Magnetoelastic Torque Sensor Utilizing a Thermal Sprayed Sense-Element for Automotive Transmission Applications*. Tech. rep. 2003-01-0711. SAE International, 2003.

[23] Chih-Jer Lin et al. *Study on Wireless Torque Measurement Using SAW Sensors*. Tech. rep. 2012.

[24] Lucefin. *X20Cr13 - 1.4021*. 2015. URL: http://www.lucefin.com/wp-content/files_mf/1.4021a420a54.pdf (visited on 04/21/2015).

[25] Steven A. Macintyre. *Magnetic Field Measurement*. Tech. rep. 1999.

[26] *Measuring Strain with Strain Gages*. 2014. URL: http://www.ni.com/white-paper/3642/en/ (visited on 04/02/2015).

[27] *MR Sensor Technology*. URL: http://www.sensitec.com/english/technology/mr-sensor-technology/mr_sensortechnologie.html (visited on 04/02/2015).

[28] Outokumpu. *Standard Cr-Ni Stainless Steels*. 2015. URL: http://www.outokumpu.com/SiteCollectionDocuments/Austenitic-Standard-Cr-Ni-Grades-Data-sheet.pdf (visited on 04/21/2015).

[29] Paul Oxley, Jennifer Goodell, and Robert Molt. “Magnetic properties of stainless steels at room and cryogenic temperatures”. In: *Journal of Magnetism and Magnetic Materials* 321 (2009).

[30] Gregory Micheal Pietron et al. *Development of Magneto-Elastic Torque Sensors for Automatic Transmission Applications*. Tech. rep. 2013-01-0301. SAE International, 2013.

[31] Research and Markets’. *Global In-vehicle Sensors Market 2014-2018*. 2014. URL: http://www.researchandmarkets.com/research/rh8msk/global_invehicle (visited on 03/29/2015).

[32] Heinrich Ruser, Uwe Tröltzsch, and Michael Horn. “Low-cost magnetic torque sensor principle”. In: *Proceedings of IEEE Sensors 2002*. Vol. 2. IEEE International, 2002.

[33] *Shaft Power Torque Meter*. URL: http://www.vaf.nl/products/overview/shaft-power-torque-meter/.

[34] *SQUID Magnetometer Sensitivity*. URL: http://hyperphysics.phy-astr.gsu.edu/hbase/hframe.htmll (visited on 04/02/2015).

[35] Lisa Tauxe. *Essentials of Paleomagnetism*. University of California Press, 2010. ISBN: 9780520260313.

[36] Vishay and Micro-Measurement. *Errors Due to Misalignment of Strain Gages*. Tech. rep.

[37] M.R. Zakaria et al. *Design and Fabrication of IDT SAW by Using Conventional Lithography Technique*. Tech. rep. 2013.